

**FACULDADE DE ENGENHARIA DA UNIVERSIDADE DO PORTO**



# **Study and Development of a Photovoltaic Panel Simulator**

Pablo González Bernal

Master in Electrical and Computers Engineering

Supervisor: Rui Esteves Araújo (PhD)

January 2012

Pablo González Bernal, 2012

# Resumo

O aumento do custo da energia das fontes convencionais e o seu impacto ambiental requer a implementação de energias renováveis, tais como a energia fotovoltaica, a qual tem aumentado exponencialmente nos últimos anos. Assim, é importante desenvolver simuladores que permitam o ensaio e a melhoria destes sistemas. A essa motivação corresponde à necessidade de dispor de um simulador capaz de testar inversores fotovoltaicos e os seus algoritmos de MPPT em condições próximas das reais.

Durante o trabalho de preparação da dissertação, vários tópicos foram endereçados, tal como os modelos dos painéis fotovoltaicos, a programação em LabVIEW e a utilização de fontes de tensão programáveis.

A parte inicial da tese é dedicada à revisão bibliográfica da energia fotovoltaica e à sua modelação. Em particular, é apresentada a base teórica dos elementos envolvidos, bem como a programação da aplicação que controla o simulador. Com isso, tornou-se possível construir uma plataforma de teste que permitiu emular um painel fotovoltaico. O simulador determina a curva característica de tensão-corrente através das informações fornecidas pelo fabricante, do nível de radiação solar e da temperatura. Da mesma forma, a aplicação fornece outras informações úteis, tais como a potência desenvolvida em qualquer instante, o fator *fill*, ou a sua eficiência para uma determinada área.

O resultado final é um emulador, que corresponde muito bem à realidade quando comparado com as curvas características fornecidas pelo fabricante do painel, e com os determinados pelo simulador.



# **Abstract**

The rising cost of conventional energy sources and their environmental impact requires the implementation of renewable energies such the photovoltaic energy, which had increased exponentially in the last years. Thus, it is important to develop emulators that allow the testing and improving these systems. The motivation corresponds to the need for a simulator able to test PV inverters and their MPPT algorithms in conditions near to real-time. During the work to prepare the dissertation, various topics regarding the photovoltaic panel, LabVIEW programming and programmable power supply were addressed. The initial part of the thesis deals with a literature review of photovoltaic energy and the model of photovoltaic array. In particular, is presented the theoretical basis of the elements involved and then deal with the programming and application development that will control the simulator. Through this, it became possible to build a test platform that allowed emulate one solar panel. The simulator calculates the voltage-current characteristic curve through the construction details of the panel, solar radiation levels and temperature. Likewise, the application provides other useful information such as the power developed at any time, the fill factor, or its efficiency in a given area.

The result is a reliable simulator, which fits very well with reality when are compared the characteristics curves provided by the manufacturer and those determined by the simulator.



# Index

<b>Resumo .....</b>	<b>iii</b>
<b>Abstract.....</b>	<b>v</b>
<b>Index .....</b>	<b>vii</b>
<b>List of Figures .....</b>	<b>ix</b>
<b>List of Tables .....</b>	<b>xi</b>
<b>Abbreviations and Symbols .....</b>	<b>xii</b>
<b>Chapter 1.....</b>	<b>1</b>
<b>Introduction .....</b>	<b>1</b>
1.1 - Analysis of Current Situation .....	1
1.2 - Objectives .....	3
1.3 - Master Thesis Structure .....	3
<b>Chapter 2.....</b>	<b>5</b>
<b>Fundamentals of Photovoltaic Energy .....</b>	<b>5</b>
2.1 - The Cell .....	6
2.1.1 - Semiconductor Limits .....	7
2.1.2 - Irradiation Limits.....	8
2.1.3 - Temperature Limits.....	9
2.2 - Types of Photovoltaic Cells.....	9

<b>Chapter 3.....</b>	<b>11</b>
<b>Modeling of solar panel .....</b>	<b>11</b>
3.1 - Electrical Model .....	11
3.1.1 - Equivalent Circuit of Two Diodes.....	11
3.1.2 - Equivalent Circuit of One Diode .....	12
3.2 - Curve Analysis.....	14
<b>Chapter 4.....</b>	<b>22</b>
<b>Software Design in Labview .....</b>	<b>22</b>
4.1 - Obtaining I-V Curve .....	22
4.2 - Power Supply .....	27
4.3 - Hardware Implementation .....	30
<b>Chapter 5.....</b>	<b>32</b>
<b>Experimental Results .....</b>	<b>32</b>
5.1 - Workplace and Switchgear Used .....	32
5.2 - User Guide .....	33
5.3 - Test Panels .....	36
5.3.1 - Sharp Electronics Corporation NU-U208FC .....	37
5.3.2 - Solarex MX-10 .....	38
5.3.3 - Solarex MX-60 .....	39
5.4 -Testing Conclusions .....	41
<b>Chapter 6.....</b>	<b>42</b>
<b>Conclusions and Future Research Areas .....</b>	<b>42</b>
6.1 - Conclusions .....	42
6.2 - Research and Improvements Areas .....	43
<b>References .....</b>	<b>44</b>
<b>Annexes.....</b>	<b>46</b>
1 - LabVIEW Block Diagram of “Without Hardware.vi”.....	47
2 - LabVIEW Block Diagram of “With Hardware.vi”.....	48

# List of Figures

<b>Figure 1.</b> Renewable Power Capacities 2010 [1].....	1
<b>Figure 2.</b> Solar PV Capacity 2010 [1].....	2
<b>Figure 3.</b> Solar PV, Existing World Capacity 1995-2010 [1] .....	2
<b>Figure 4.</b> Master Thesis Structure .....	4
<b>Figure 5.</b> Off-grid PV System [2].....	5
<b>Figure 6.</b> Band Gap in Semiconductors [3] (edited).....	6
<b>Figure 7.</b> Photovoltaic Cell Scheme .....	6
<b>Figure 8.</b> The Shockley-Queisser Limit or the Efficiency of a Solar Cell [3] (edited) .....	7
<b>Figure 9.</b> Breakdown of the Causes for the Shockley-Queisser limit [4] (edited).....	7
<b>Figure 10.</b> Solar Radiation Spectrum [5] (edited) .....	8
<b>Figure 11.</b> Best Research-Cell Efficiencies [6] .....	10
<b>Figure 12.</b> Two diode equivalent circuit of a PV cell .....	11
<b>Figure 13.</b> One diode equivalent circuit of a PV cell .....	12
<b>Figure 14.</b> A Typical current-voltage I-V curve for a solar cell .....	14
<b>Figure 15.</b> A Typical power-voltage P-V curve for a solar cell .....	15
<b>Figure 16.</b> I-V characteristic as a function of irradiance.....	16
<b>Figure 17.</b> P-V characteristic as a function of irradiance .....	16
<b>Figure 18.</b> I-V characteristic as a function of operating temperature .....	17
<b>Figure 19.</b> P-V characteristic as a function of operating temperature .....	17
<b>Figure 20.</b> I-V characteristic as a function of diode quality factor.....	18
<b>Figure 21.</b> P-V characteristic as a function of diode quality factor .....	18
<b>Figure 22.</b> I-V characteristic as a function of series resistance.....	19

<b>Figure 23.</b> P-V characteristic as a function of series resistance .....	19
<b>Figure 24.</b> I-V characteristic as a function of the number of cells in series .....	20
<b>Figure 25.</b> P-V characteristic as a function of the number of cells in series .....	20
<b>Figure 26.</b> I-V characteristic as a function of the number of cells in parallel .....	21
<b>Figure 27.</b> P-V characteristic as a function of the number of cells in parallel.....	21
<b>Figure 28.</b> Inputs and outputs of the Matlab simulator .....	23
<b>Figure 29.</b> SubVI 1 .....	25
<b>Figure 30.</b> SubVI 2 .....	26
<b>Figure 31.</b> SubVI 3 .....	26
<b>Figure 32.</b> SubVI 4 .....	26
<b>Figure 33.</b> Algorithm Used to Obtain the IV Curve .....	27
<b>Figure 34.</b> Output of a Constant-Voltage (left) and Constant-Current (right) Supply .....	28
<b>Figure 35.</b> Output Characteristic of a Constant-Voltage/Constant-Current Supply.....	28
<b>Figure 36.</b> Philips-Fluke PM2832 Power Supply .....	29
<b>Figure 37.</b> Philips-Fluke PM2832 Power Supply Detail .....	29
<b>Figure 38.</b> Algorithm Used to Set the Power Supply .....	30
<b>Figure 39.</b> SubVI 5 .....	31
<b>Figure 40.</b> Resistance Line .....	31
<b>Figure 41.</b> Connection Scheme .....	32
<b>Figure 42.</b> Workplace.....	33
<b>Figure 43.</b> LabVIEW Front Panel of “With Hardware.vi” .....	34
<b>Figure 44.</b> SHARP UN-U208FC from Data-Sheet [7] .....	37
<b>Figure 45.</b> SHARP UN-U208FC for Different Irradiances from Simulator .....	37
<b>Figure 46.</b> Solarex MSX-10 for STC from simulator .....	38
<b>Figure 47.</b> Solarex MSX-10 for different temperatures from datasheet [8].....	39
<b>Figure 48.</b> Solarex MSX-10 for different temperatures from simulator.....	39
<b>Figure 49.</b> Solarex MSX-60 for 100W/m <sup>2</sup> from simulator .....	40
<b>Figure 50.</b> Solarex MSX-60 for STC from simulator .....	40
<b>Figure 51.</b> Example of a Photovoltaic Test System [10].....	43

# List of Tables

<b>Table 1.</b> Diode quality factor and band gap voltage .....	36
<b>Table 2.</b> Experimental Results for SHARP UN-U208FC .....	37
<b>Table 3.</b> Experimental Results for Solarex MSX10 .....	38
<b>Table 4.</b> Experimental Results for Solarex MSX60 .....	41

# Abbreviations and Symbols

Nomenclature	Meaning
$G_a$	Environmental irradiation ( $\text{W}/\text{m}^2$ )
$I_D$	Diodo current branch (A)
$I_L$	Photocurrent (A)
$I_{SH}$	Rsh current branch (A)
$I_{sc}$	Short circuit current (A)
$I_0$	Diode saturation current (A)
$P_{max}$	Maximum power (W)
$R_{SH}$	Parallel resistance ( $\Omega$ )
$R_s$	Series resistance ( $\Omega$ )
$V_g$	Band gap voltage (eV)
$V_{oc}$	Open circuit voltage (V)
$V_t$	Thermal voltage (V)
A	Cell area ( $\text{m}^2$ )
G	Irradiance, Suns ( $\text{W}/\text{m}^2$ )
I	Load current (A)
K	Boltzmann constant ( $1,38065 \times 10^{-23} \text{J}/\text{K}$ )
n	Diode quality factor (Between 1 y 2)
$\eta$	Maximum efficiency (%)
q	Electron charge ( $1,602 \times 10^{-19} \text{C}$ )
T	Operating temperature (K)
V	Load voltage (V)
FF	Fill factor (%)

# Chapter 1

## Introduction

### 1.1 - Analysis of Current Situation

The increasing cost of conventional energy sources and their environmental impact suggests an increasing penetration of renewable energies in the field of electricity production. This is already a reality, since about half of all new power plants in the world produce electricity from renewable energy. Although this does not seem to be enough because in 2010 the world reached a record high of 10,000 million tons of CO<sub>2</sub>, which means an increase of 49% over the past two decades, according to report in the journal Nature Climate Change. (Fig.1)



Figure 1. Renewable Power Capacities 2010 [1]

Still, 2010 was an extraordinary year for photovoltaic, only between 2009 and 2010 the installed capacity grew by 72% [1]. Photovoltaic again demonstrated its ease and speed of deployment, reaching more than 2,100 MW connected only during the month of June in 2010 in Germany.

Germany is the country added more capacity in PV in 2010, followed by Italy, Czech Republic, Japan and the United States. Germany is also the country with the largest installed capacity of PV (44%), followed by Spain (10%), Japan (9%), Italy (9%) and USA (6%). Europe, as you can see, accounts for over 75% of global installed capacity of PV. (Fig.2)

In total, the new capacity installed in 2010, the volume of the accumulated total power is on the edge of adding the 40,000 MW. At the beginning of the decade, in 2000, the total power installed globally was only of 1,500 MW.

Also in 2010, became the first renewable power in Europe, with a 22% share, ahead of the wind (17%) and second only to the gas (52%). In total, photovoltaic now account for 3% of the installed power in the EU. Yet all renewable sources (excluding the large-scale hydropower) contributed only 3.3% of global electricity production.

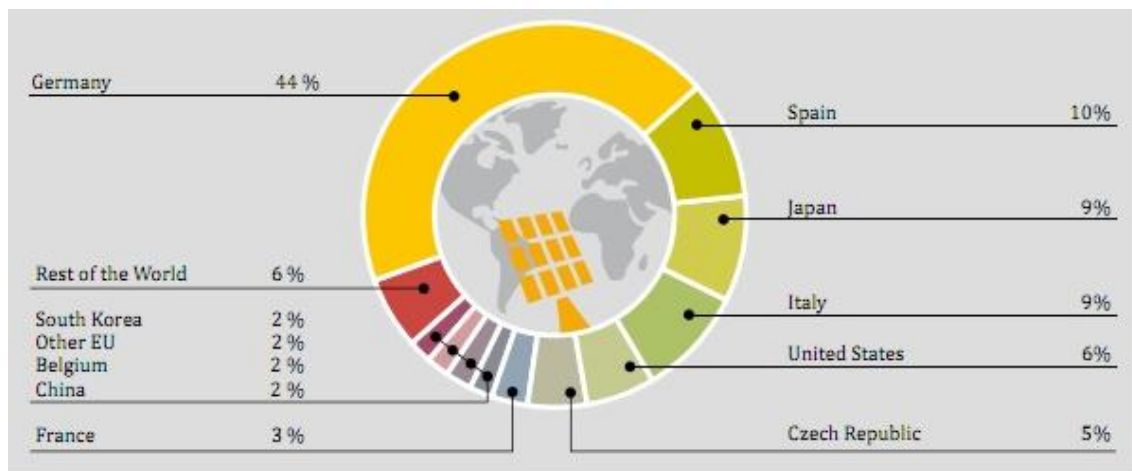


Figure 2. Solar PV Capacity 2010 [1]

The PV power installed capacity by 2010 is 40 GWp (+17 GWp compared to 2009). Was planned for November 2011 to install over 24 GW, so the global capacity will now be exceeded more than 64 GW. Photovoltaic energy is still the fastest growing renewable annual average between 2005 and 2010 (49%). (Fig. 3)

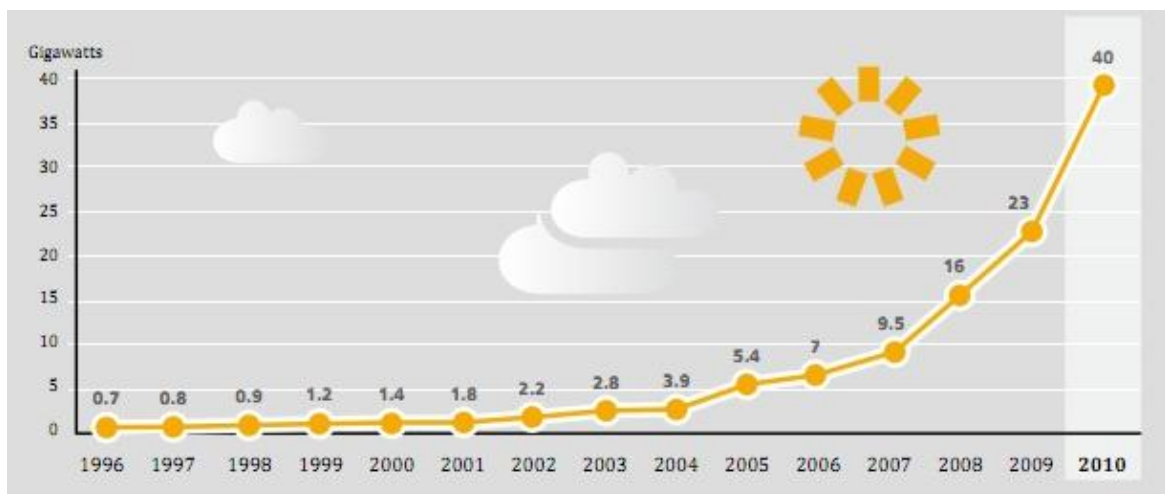


Figure 3. Solar PV, Existing World Capacity 1995-2010 [1]

In a short term is expected that photovoltaic energy will be one of the fastest-growing market. This growth creates new problems for manufacturers since testing a large number of photovoltaic modules before installation is complicated.

Currently testing for the connected equipment, such as inverters, we use a real panel. This leads to a problem, since the oscillations of temperature and radiation is difficult to isolate the variables that affect the panel performance.

Using a programmed voltage source, the testing procedures can be performed using constant values of both voltage and current. But this is not entirely similar to the operation of the panel, since it does not take into account climatic conditions.

The simulator developed, would be the midpoint in order to perform these measurements, based on the characteristics of the panel, radiation and temperature, but giving constant values of voltage and current. So this simulator is a more sophisticated system than the other two, in order to identify the inverters needed for installation.

The user then can identify the factors that affect performance of the panel, analyzing the resulting curve by changing variables. Thus, it is also more accurate measurements made in other components connected to the photovoltaic panel.

This simulator allows you to test hundreds of panels without having to purchase them, besides being able to control their response to different conditions of temperature and radiation.

## 1.2 - Objectives

The ultimate goal of this thesis is to build a solar panel emulator in the LabVIEW programming environment. This has been developed the following steps:

1. Understand the patterns and factors that affect the behavior of the photovoltaic cell
2. Determine the current-voltage curve dependence of on these factors
3. Controlling a power source following the I-V characteristic curve
4. Conclusions and proposals for future research
5. Make a project report and publish it on the web

## 1.3 - Master Thesis Structure

This master thesis is within the area of alternative energies, focusing the same in the study and development of a computational tool aiming to simulate the PV modules performance under different operating conditions resulting from different levels of temperature and radiance. The first chapter is an introduction that shows a general analysis of the situation nowadays in the market of photovoltaic systems. In addition they are marked

the desired objectives of the thesis. The second chapter studies the general functioning and the limits of the photovoltaic cell, to enter in the third chapter to capture this operation in his electrical equivalent circuit, and analyze the variables that affect the behavior of the cell through the study of the I-V and P-V characteristic curves.

After the presentation of the basics of the photovoltaic cell, the Chapter 5 and Chapter 6 deal with the theoretical and practical development of the simulator, there is detailed and discussed all the work done through the program LabVIEW and shows the result obtained by the experimentation. The structure of the document is shown in figure 4.

Finally the chapter 6 contains conclusions and future research areas.

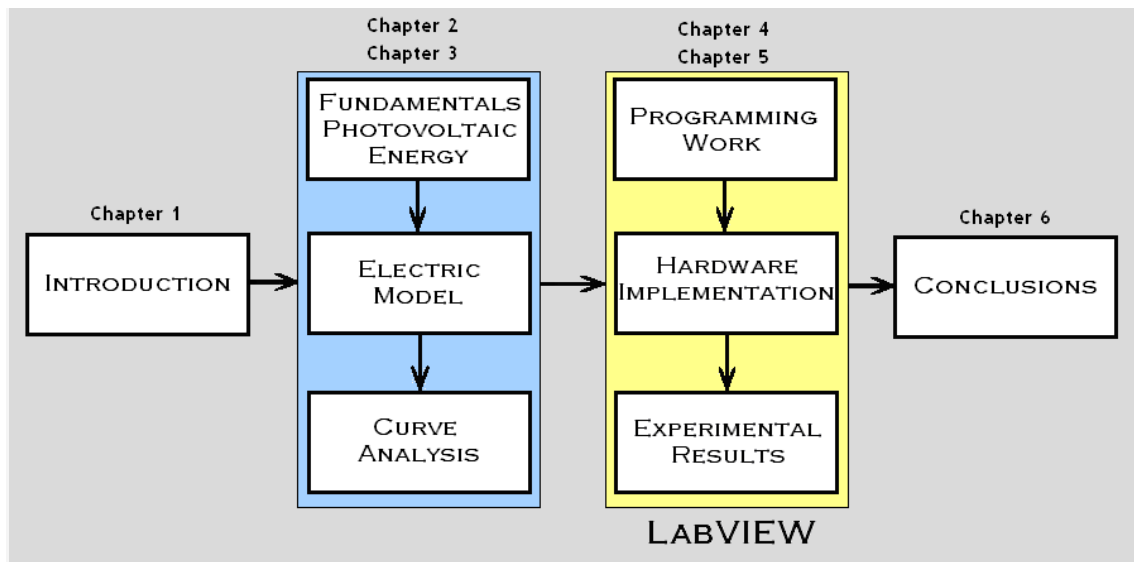


*Figure 4. Master Thesis Structure*

## Chapter 2

# Fundamentals of Photovoltaic Energy

The photovoltaic effect is the electrical potential developed between two different materials when their common junction is illuminated by photon irradiation. In other words, photovoltaic solar energy is the use of electromagnetic radiation of the sun shining on a photovoltaic cell produces electricity in a direct way. The solar cell is composed of a semiconductor material, usually silicon, which when crossed by the photons generated in one side an electric current produced by the photovoltaic effect.

The manufacture of these cells is expensive in both time and money, although silicon with which they are made is very abundant in the earth; its procedure is laborious and complicated.

These cells are combined in series to increase voltage (V) or parallel to increase current without increasing voltage. The current generated is stored in batteries and converted to AC through inverters. (Fig. 5)

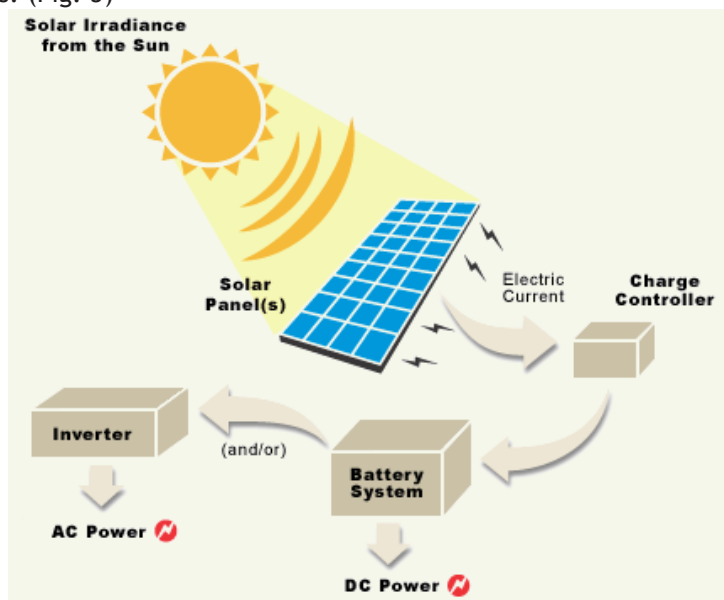


Figure 5. Off-grid PV system [2]

## 2.1 - The Cell

Much of the electrical characteristics of photovoltaic solar cells depend on the physical properties of semiconductor materials used in its manufacture, and industrial processes applied.

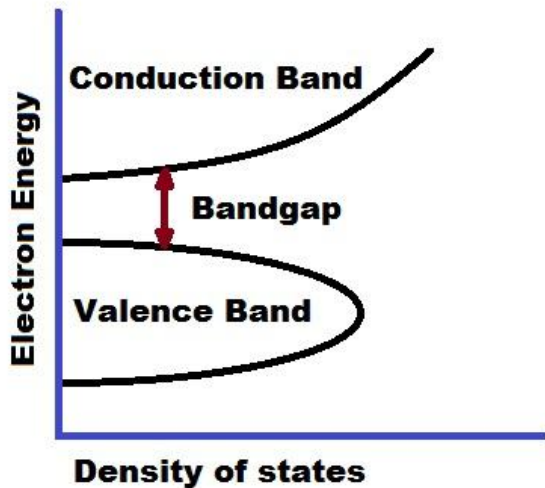


Figure 6. Bandgap in semiconductor [3] (edited)

At the junction photovoltaic cells is the most widely used pn junction in which the band gap ( $E_g$ ) of semiconductor materials is the same. By combining both types of materials the diffusion of electrons in the p lead to the recombination of electrons and holes, causing the appearance of negatively charged ions in this area. The loss of negative charge (electrons) in n-type material near the joint area will generate positive ions.

When a photon is absorbed by a semiconductor material, increases the energy of the valence band electrons, and makes the jump into the conduction band, resulting in free electrons. This occurs when the incident photon energy is greater than the band gap semiconductor. (Fig. 6)

Upon this jump, the holes generated in the crystal lattice, the burden associated with these gaps should be the same as the electron but of opposite sign, thus creating hole-electron pair.

At the junction photovoltaic cells is the most widely used pn junction in which the band gap ( $E_g$ ) of semiconductor

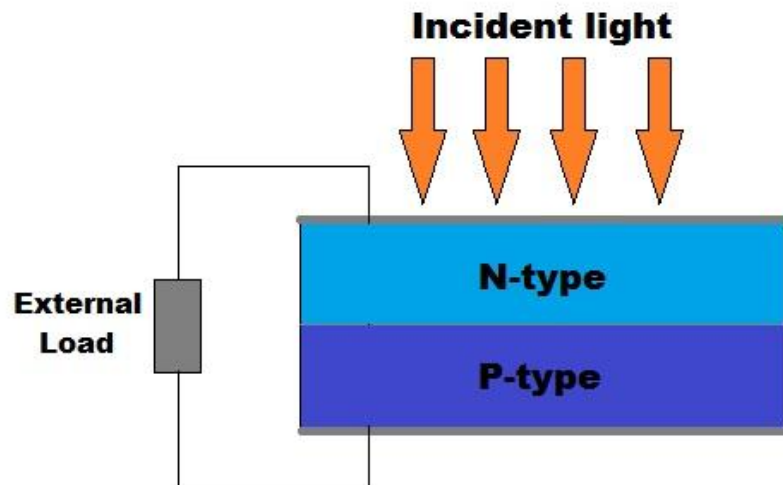


Figure 7. Photovoltaic cell scheme

Both types of ions form an electrical potential barrier and therefore a current that is proportional to the incidence of radiation. The cell behavior is very similar to the classic p-n junction diode. (Fig. 7)

### 2.1.1 - Semiconductor Limits

The solar panel efficiency, is largely determined by the type of doping material and the band gap of the semiconductor.

Shockley-Queisser limit refers to the theoretical maximum efficiency can be obtained from a solar cell that uses a p-n junction. (Fig.8)

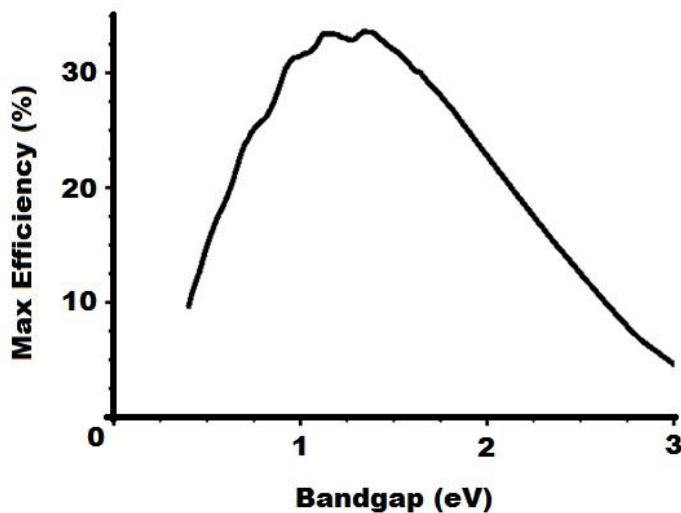


Figure 8. The Shockley-Queisser limit for the efficiency of a solar cell. [3] (edited)

The causes of Shockely-Queisser limit is indicated in the figure. The orange area is the useful power, the red area is the energy of below-band gap photons, the green height is energy lost when hot photo generated electrons and holes relax to the band edges, the blue zone is energy lost in the tradeoff between low radioactive recombination versus high operating voltage. (Fig.9)

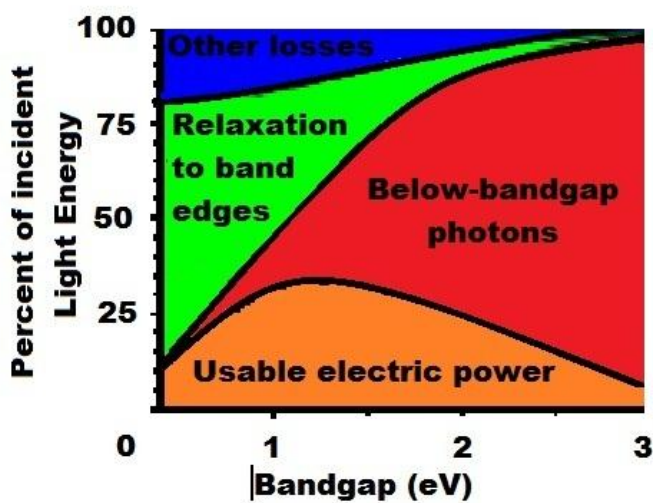


Figure 9. Breakdown of the causes for the Shockley-Queisser limit. [4] (edited)

## 2.1.2 - Irradiation Limits

The amount of current generated in the PV is affected by two variables: the intensity of incident light and the wavelength of the incident rays.

Each semiconductor material shall have a limited absorption of radiation. Below this, no electrons make the photovoltaic effect. The energy of a photon is determined by the wavelength but not by the intensity of light, against shorter, have more energy.

Increasing light intensity increases proportionally photoelectron emission rate in the photovoltaic material. Solar cells are usually coated with an anti-reflective material to capture the maximum amount of radiation possible.

Below is a graph where we can see the range that can take advantage of a silicon photovoltaic cell. (Fig.10)

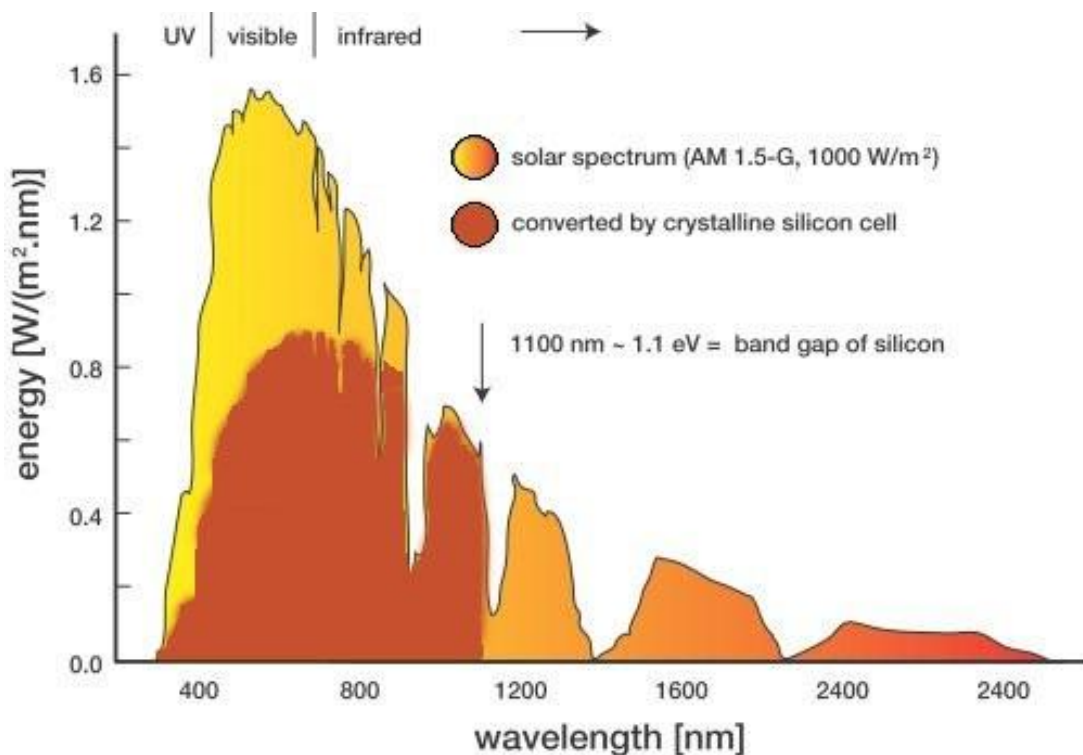


Figure 10. Solar radiation Spectrum [5] (edited)

Photons with wavelengths too high will pass through the panel in the form of heat. Photons with a wavelength less than 1.100nm have more energy than the required to separate the electron, the excess energy is converted to heat losses.

### 2.1.3 - Temperature Limits

As the temperature rises above the absolute zero the number of electrons that jump to the conduction band free electrons increase due to thermal ionization phenomenon.

The panel exposure to sunlight causes the increase of temperature of the cells representing a small increase in intensity because the band gap decreases with temperature. Yet at the same time there is a larger decrease in the value of the voltage, because it is maximum, and of equal value than the band gap when the temperature is absolute zero. So the overall effect is the reduction of the power supplied by the panel.

The power will therefore increase with increasing radiation and lower temperature.

## 2.2 - Types of Photovoltaic Cells

There are commercially available several types of PV cells. Here it is given a brief explanation of what are their main advantages and disadvantages. Currently are emerging continuously new technologies to market, so here it will not appear all that exist, but the best known.

**Monocrystalline Silicon:** Sections are based on a perfectly crystallized silicon bar in one piece. Efficiency above 24% in laboratory, but in reality, commercial panels are around 15% [23]. They are more expensive, heavier and more fragile to shocks.

**Polycrystalline Silicon:** The crystallization process of silicon is different from before. Sections are based on a silicon bar that is structured as small disordered crystals. These cells present an efficiency of up to 19% in the laboratory, and about 14% in the modules market [23]. The cost is lower than the monocrystalline, so that their efficiency is more profitable.

**Thin-film Solar Cell (TFSC):** They are manufactured by placing a thin film photovoltaic material on a wide variety of surfaces. These are less efficient and less costly to produce than the previous two types. These solar panels are built in roll form eliminating many costly processes involved in manufacturing of the conventional panels. These cells are categorized according to the photovoltaic material used:

**Amorphous Silicon:** They not follow any crystal structure. His power is reduced over time, especially during the first months, after which are basically stable. They are used for small electronic devices. These cells present in the laboratory efficiencies of up to 13%, with commercial modules of about 8% [23].

**Cadmium Telluride:** It is usually sandwiched with cadmium sulfide to form a p-n junction photovoltaic solar cell. CdTe cells use a n-i-p structure. Laboratory performance 16% and 8% commercial modules [23].

**Copper Indium Diselenide:** Laboratory performance close to 17% and 9% commercial modules [23].

**Dye-sensitized Solar Cell:** It is based on a semiconductor formed between a photo-sensitized anode and an electrolyte, a photo electrochemical system.

**Gallium Arsenide:** One of the most efficient, consisting of a mixture of gallium and arsenic. Gallium is a byproduct of the smelting of other metals such as aluminum and zinc. Laboratory performance of 25.7% and 20% commercial modules [23].

**Multi-junction or Tandem Cells:** Are solar cells that contain multiple pn junctions. Each union is set to a different wavelength, reducing a major source of losses and increasing efficiency. Currently, the best examples of laboratory silicon solar cells have an efficiency of traditional about 25%, while examples of laboratory multi-junction cells have demonstrated superior performance to 42% [23].

Given the diode quality factor and the band-gap voltage of the semiconductor material, the simulator will have no problem to emulate all types of cells in the market. (Fig. 11)

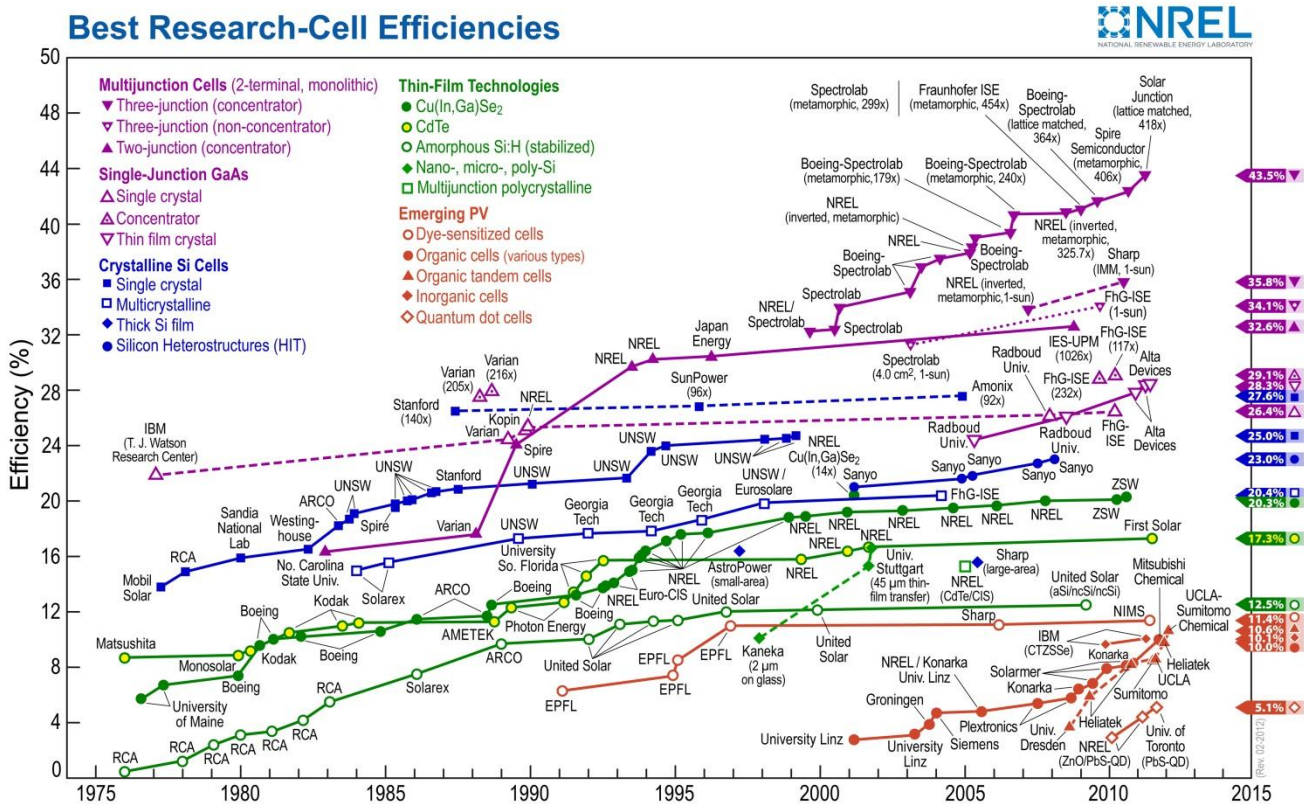


Figure 11. Best Research-Cell Efficiencies [6]

# Chapter 3

## Modeling of photovoltaic panel

### 3.1 - Electric Model

This section formulates the model of a photovoltaic isolated cell. To understand the behavior of a solar cell, it is useful use an equivalent electrical model, based on well-known electrical components. An ideal cell can be modeled as a current supply connected in parallel to a diode. The PV simulator must have a current and output voltage given by the diode equivalent model, as close as possible to the real system, or to the characteristics provided by manufacturers.

#### 3.1.1 - Equivalent circuit of two diodes [16]

The most complete model consists of a current source whose intensity  $I_L$  is directly proportional to radiation  $G$ , in parallel with two diodes, one that simulates the diffusion of minority charge and the other corresponding to the recombination of the junction. The parallel resistance  $R_{sh}$  represents the leakage current losses, and the series resistor  $R_s$  represents the internal losses of the cell, the heat losses by Joule effect due to current flow, impurities and losses among cell connections. (Fig.12)

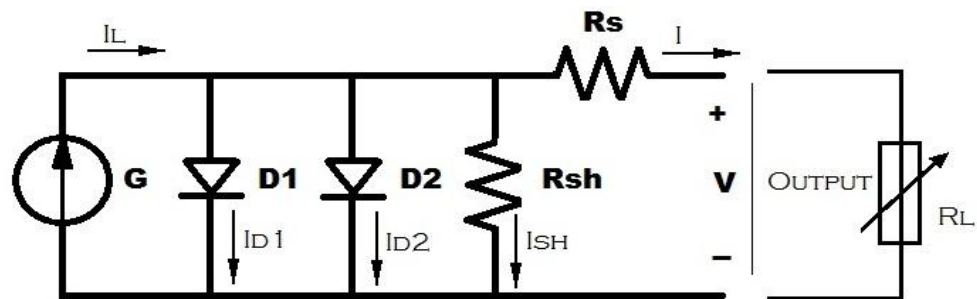


Figure 12. Two diode equivalent circuit of a PV cell

$$I = I_L - I_{D1} - I_{D2} - I_{SH} \quad (3.1)$$

$$I = I_L - I_{0D1} \left( e^{\frac{q(V+R_S \cdot I)}{n_1 \cdot K \cdot T}} - 1 \right) - I_{0D2} \left( e^{\frac{q(V+R_S \cdot I)}{n_2 \cdot K \cdot T}} - 1 \right) - \frac{V + R_S \cdot I}{R_{SH}} \quad (3.2)$$

### 3.1.2 - Equivalent circuit of one diode [17]

The model that will work is a simplified version of this but that fits quite well to reality, and greatly facilitates the process of computing and programming. In this ideal model the current source and the diode represent the conversion of solar energy in electric energy.

The simplified model is based on a current source in parallel with a diode, and only taken into account the series resistance  $R_s$ .  $R_{sh}$  value usually has a very high value, more than 200 Ohms, and our hypothesis, we despise, since the panel efficiency is insensitive to changes in  $R_{sh}$ . (Fig. 13)

In an ideal cell  $R_s = 0$  (there will be no voltage drop before the load) and  $R_{sh} = \infty$  (no other roads where you can lose part of the current).

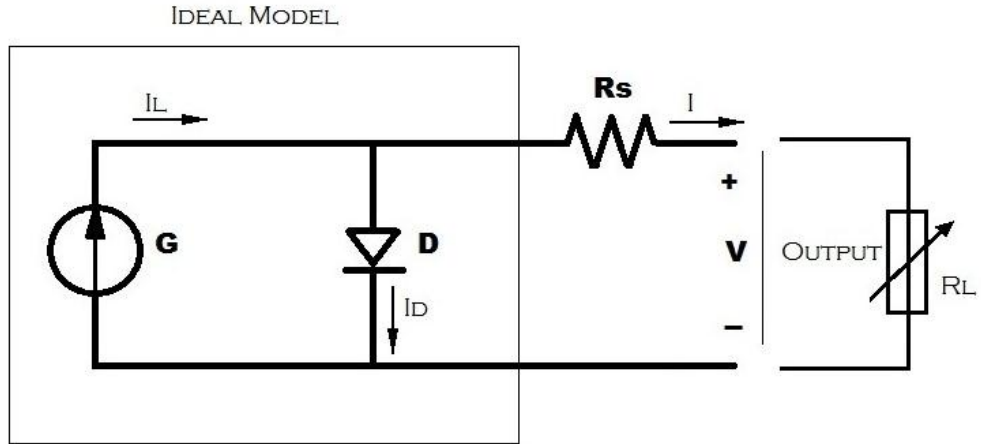


Figure 13. One diode equivalent circuit of a PV cell

$$I = I_L - I_D \quad (3.3)$$

$$I = I_L - I_0 \left( e^{\frac{q(V+R_S \cdot I)}{n \cdot K \cdot T}} - 1 \right) \quad (3.4)$$

The saturation current of the diode and the photocurrent depend with the temperature. The following equations consider the radiation and temperature as parameters that affect the behavior of the panel [17].

$$I_L = I_L(T_1) + K_0(T - T_1) \quad (3.5)$$

$$I_L(T_1) = I_{SC}(T_{1nom}) \frac{G}{G_{nom}} \quad (3.6)$$

$$K_0 = \frac{I_{SC}(T_2) - I_{SC}(T_1)}{(T_2 - T_1)} \quad (3.7)$$

$$I_0 = I_0(T_1) \left( \frac{T}{T_1} \right)^n e^{-\frac{q \cdot V_g(T_1) \cdot \left( \frac{1}{T} - \frac{1}{T_1} \right)}{nK}} \quad (3.8)$$

$$I_0(T_1) = \frac{I_{SC}(T_1)}{\left( e^{\frac{qV_{oc}(T_1)}{nKT_1}} - 1 \right)} \quad (3.9)$$

Equation 3.10 represents the series resistance inside each cell in the connection between cells and the internal losses. The series resistance will vary with the temperature since equation 3.11 depends on the saturation current of the diode.

$$R_s = -\frac{dV}{dI_{Voc}} - \frac{1}{X_v} \quad (3.10)$$

$$X_V = I_0(T_1) \frac{q}{nKT_1} e^{\frac{qV_{oc}(T_1)}{nKT_1}} \quad (3.11)$$

The model takes two fixed values of temperature to calculate the output parameters of the panel at the operating temperature.

The short circuit current will occur when  $R_L = 0$  in totally lighting conditions, with  $V=0$ , there is the maximum current.

$$I_L = I_{sc} \quad (3.12)$$

The open circuit voltage will occur when  $R_L = \infty$ , with  $I = 0$ , all the photocurrent through the diode, and it produces the maximum voltage value. In the darkness, the characteristic curve of the photovoltaic cell is very similar to the exponential curve of a diode.  $V_{oc}$  represents the voltage of the cell in the dark.

$$V_{oc} = \frac{nKT}{q} \ln \left( \frac{I_L}{I_D} \right) = V_t \ln \left( \frac{I_L}{I_D} \right) \quad (3.13)$$

$$V_t = \frac{nKT}{q} \quad (3.14)$$

When the cell works in the  $I_{sc}$  and  $V_{oc}$  points, the power developed by the panel will be zero. The maximum power dissipated by a resistive load connected to the panel is easily calculated by the equation.

$$P_{max} = V_{max} \cdot I_{max} \quad (3.15)$$

**Fill Factor (FF):** Is another interesting parameter to study the behavior of a solar cell. It expresses the ratio between the maximum power point and the product of the open circuit voltage and short circuit current is a way of measuring the quality of the photovoltaic cell.

$$FF = \frac{V_{max} \cdot I_{max}}{V_{oc} \cdot I_{sc}} \quad (3.16)$$

Maximum efficiency is the ratio enters the maximum power and power of the incidence of light.

$$\eta = \frac{V_{max} \cdot I_{max}}{A \cdot G_a} \quad (3.17)$$

### 3.2 - Curve analysis

The electrical characteristics of the cell are represented through their I-V and P-V curves. First explains the IV curve and the PV curve, then how these vary with the change of radiation, temperature, diode quality factor, series resistance, and coupling of more cells either connected in series or in parallel.

Connecting the simulator to a resistive load, his property meets Ohm's law ( $I/V = 1/R$ ) in this way the power generated by the panel depends only on the value of the resistance. (Fig. 14)

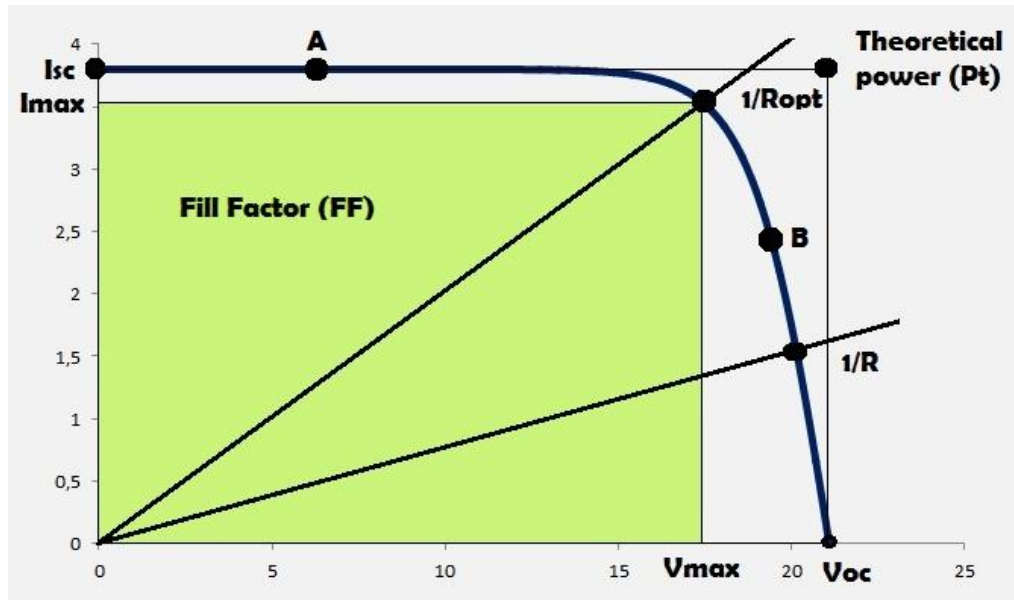


Figure 14. A Typical current-voltage I-V curve for a solar cell

If  $R$  is small, the panel will work in the point A, to the left of the maximum power point, where you have a behavior similar to a current source. If  $R$  is close to zero, the panel will work on short circuit  $I_{sc}$  point where no power is generated.

If  $R$  is large the panel will work in the point B to the right of maximum power point, where you have a behavior similar to a voltage source. If  $R$  approaches infinity, work on open circuit  $V_{oc}$  point where not produce any power. There will be an optimal  $R$  where the panel develops maximum power, which is calculated by the fill factor, which can be seen graphically as the ratio of green area ( $P_{max} = I_{max} \cdot V_{max}$ ) for the white area ( $P_t = V_{oc} \cdot I_{sc}$ ).

The PV curve is the product of voltage and output current. The PV systems are designed to work near the knee, slightly to the left side. (Fig.15)

Most manufacturers of inverters for photovoltaic plants make a wide range between the maximum power point of maximum and minimum ( $V_{ppmax}$ ,  $V_{ppmin}$ ), where the inverter acts properly, and has no problem to find the maximum power point in where the panel is working. In addition will also point  $V_{omax}$ ,  $V_{omin}$  and where the inverter can work and a value of  $V_{dcmax}$  which must not be exceeded, even under open circuit and the minimum temperature of the PV module.

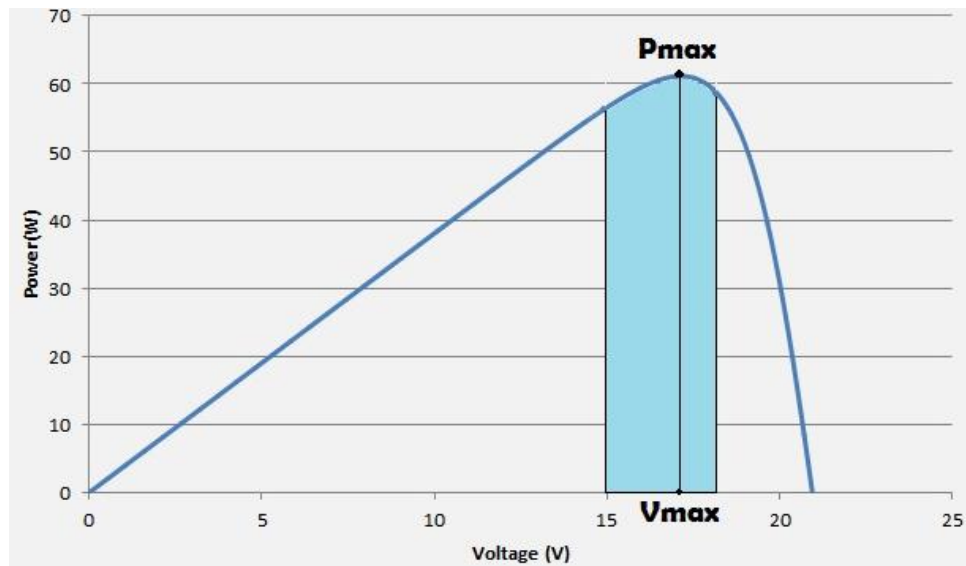


Figure 15. A Typical power-voltage P-V curve for a PV module

For practical applications the question arises at which values of  $V_{mpp}$  an inverter should reasonably be tested and which interval the STC\* array voltages  $V_{mpa-stc}$  and  $V_{oca-stc}$  of the PV plant should be chosen. The simulator can calculate the maximum power point of the photovoltaic module chosen, with the desired environmental conditions. Thus, you can connect the inverter to the power source programmed and analyze his behavior.

The following graphics are made with the application developed in LabVIEW without hardware, and then exported to an Excel workbook to improve its design and understanding.

The panel chosen for the analysis of curves is the MX-60. The starting parameters used are for the standard conditions STC\*.

Later we will analyze the process carried out to program the software.

---

\*STC: Standard Conditions for testing panels: solar radiation of 1000 W / m<sup>2</sup>, PV cell temperature 25 ° C, spectral value = 1.5 AM. It should be noted that the radiation is almost always less than 1000 Watts / m<sup>2</sup>, the temperature often exceeds 25 ° C, while the spectral value can vary between 0.7 (high above sea level) and very large values.

The (Fig.16) and (Fig.17) show the dependence of the photovoltaic cells as a function of incident solar irradiance. The curves correspond to  $1000 \text{ W/m}^2$ ,  $750 \text{ W/m}^2$ ,  $500 \text{ W/m}^2$ ,  $250 \text{ W/m}^2$  at  $25^\circ\text{C}$ . It is noted, of course, that with increasing incident light power, more power is generated.

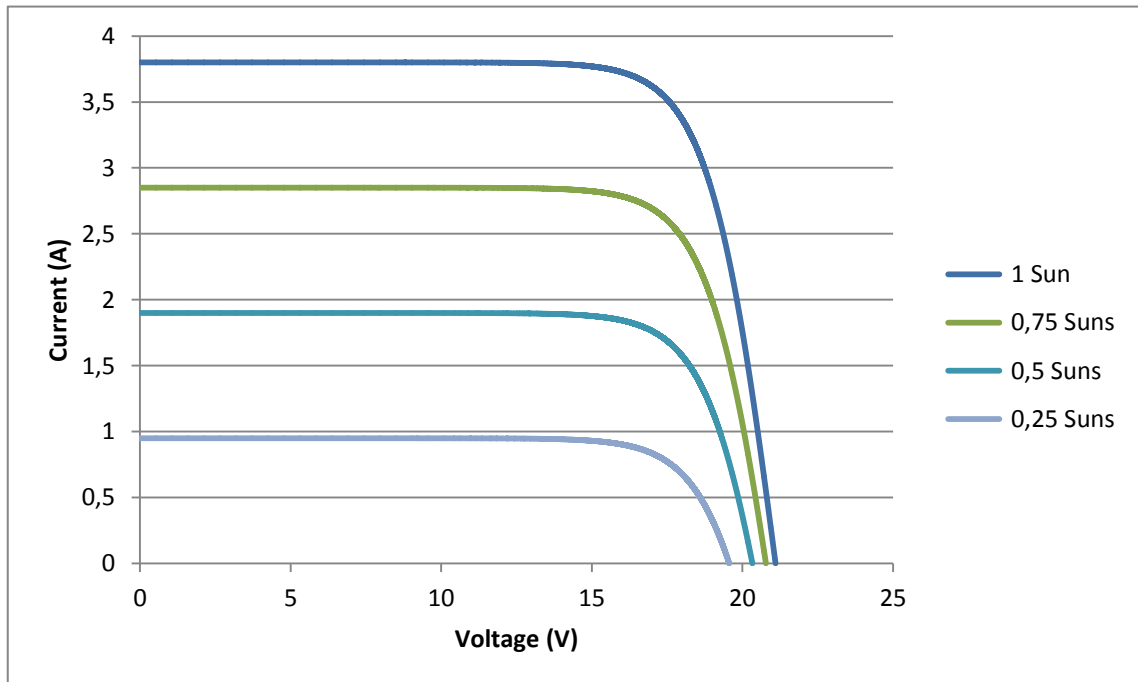


Figure 16. I-V characteristic as a function of irradiance

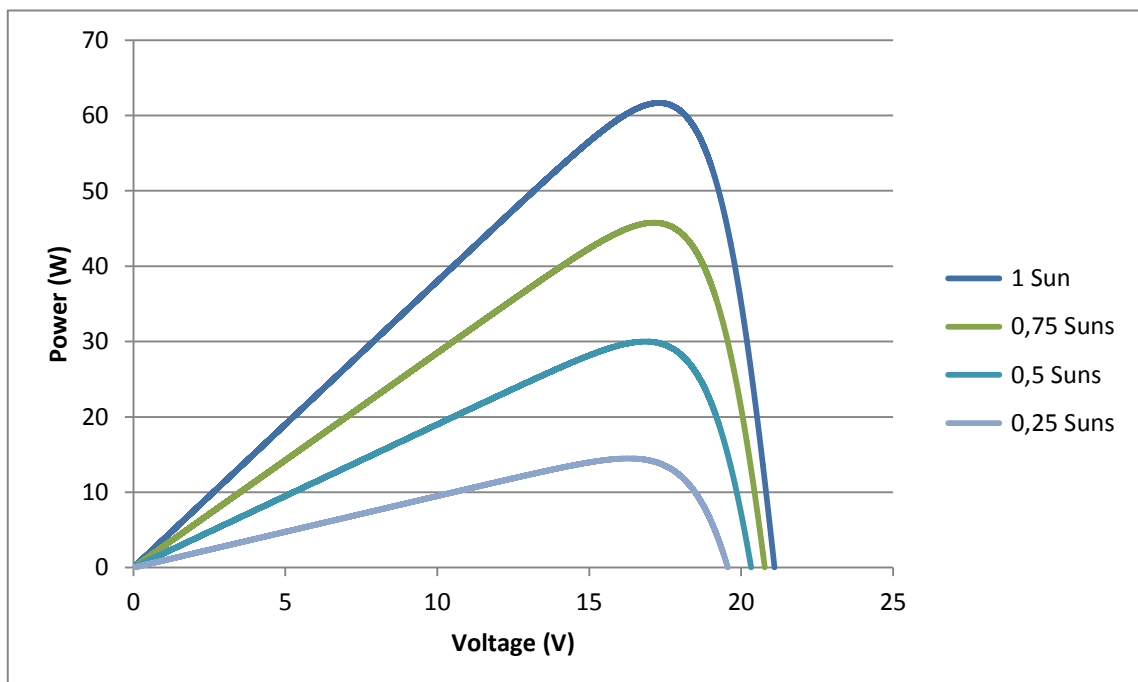


Figure 17. P-V characteristic as a function of irradiance

In (Fig.18) and (Fig.19) make sure that the temperature adversely affects the power of the cell, because even slightly increase the intensity, voltage loss is more pronounced.

This effect is observed in the hour of greatest irradiance, the power decreases slightly due to increased temperature.

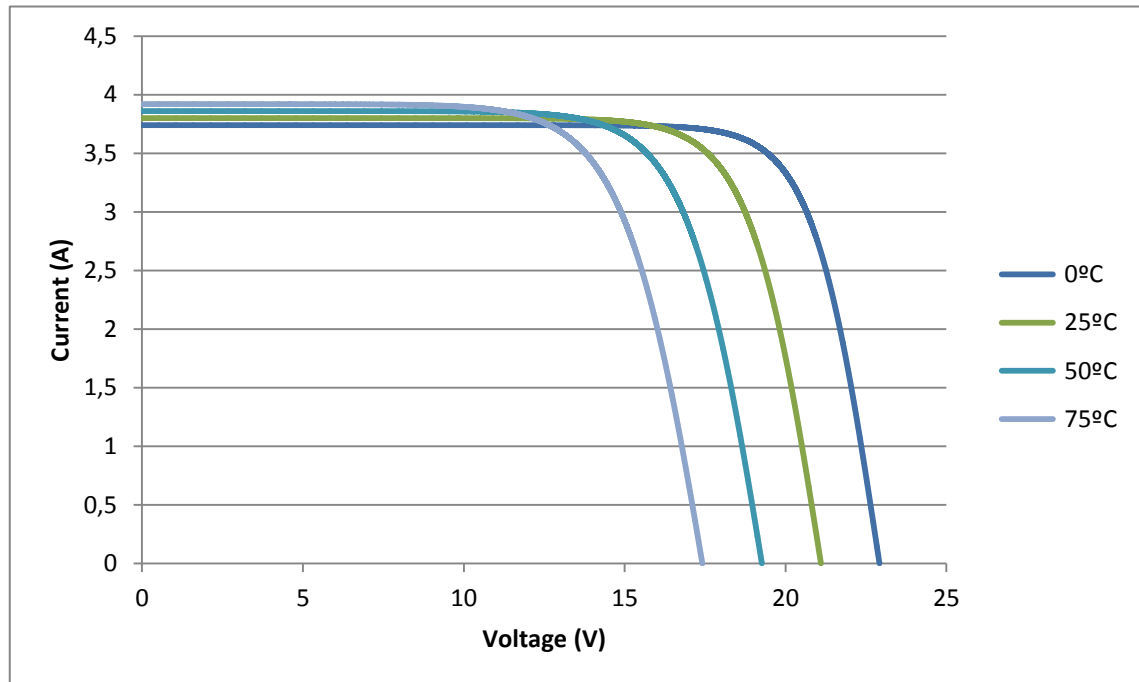


Figure 18. I-V characteristic as a function of operating temperature

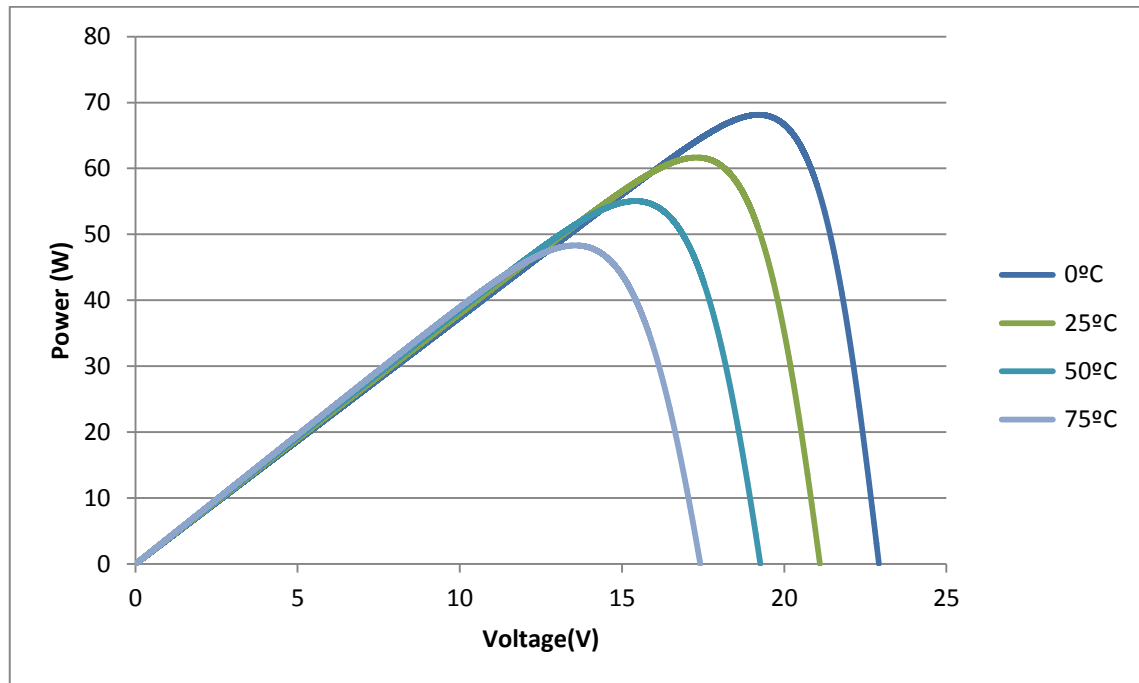
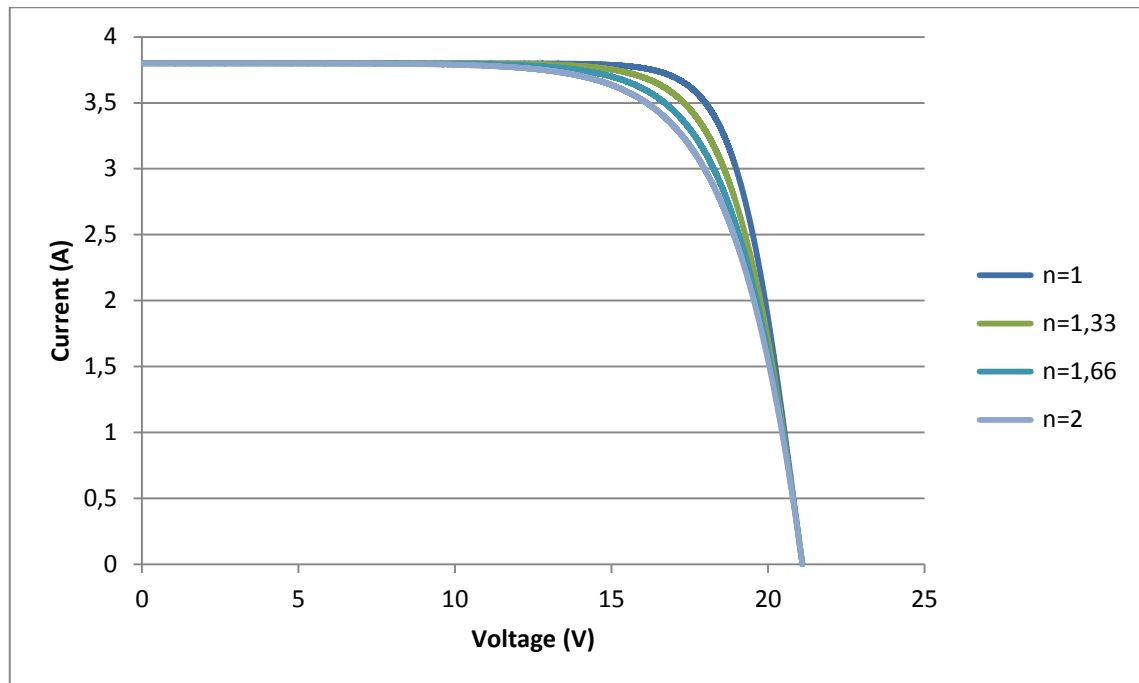
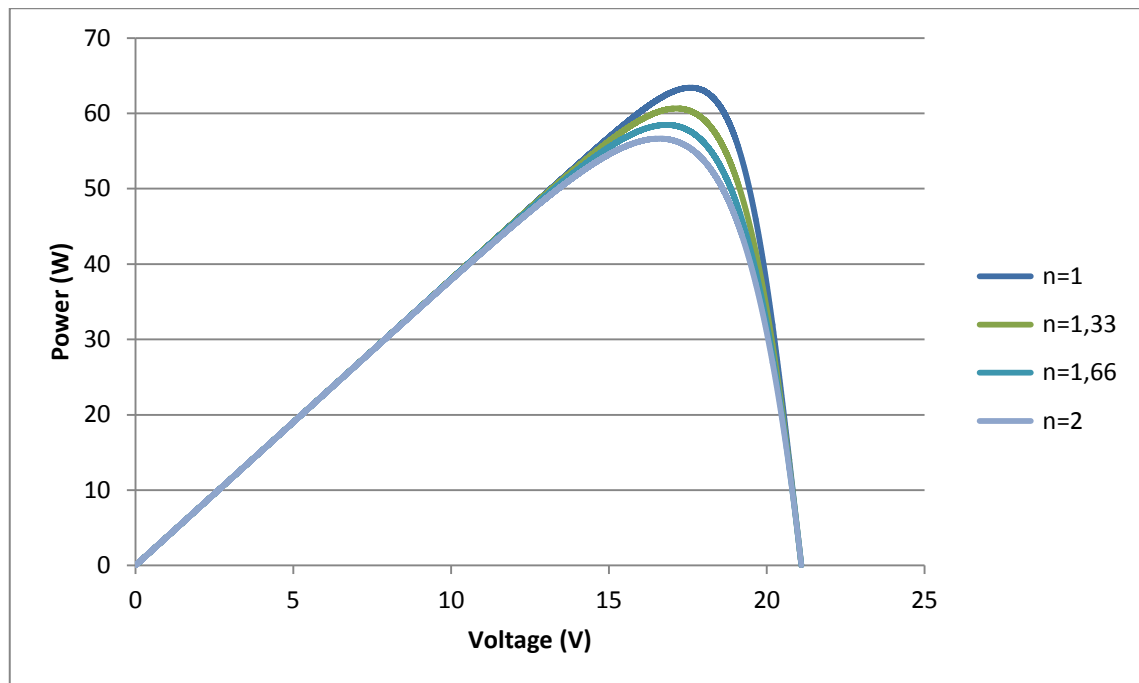


Figure 19. P-V characteristic as a function of operating temperature

The ideality factor, also known as the quality factor varies from 1 to 2 depending on the fabrication process and semiconductor material, see in (Fig.20) and (Fig.21) Show that with increasing the diode quality factor reduces the maximum power that the panel could provide. In addition, deteriorating fill factor, because although  $I_{sc}$  and  $V_{oc}$  does not change, if it does the curvature of the knee where the maximum power occurs.



*Figure 20. I-V characteristic as a function of diode quality factor*



*Figure 21. P-V characteristic as a function of diode quality factor*

The (Fig.22) and (Fig.23) show the effect of the series resistance. As the value of the resistor in series increases it degrades the performance of the cell.

The resistive behavior tends to change the curve of the diode, resulting in the above case as a decline in both the power and fill factor, regardless of  $I_{sc}$  and  $V_{oc}$  not change.

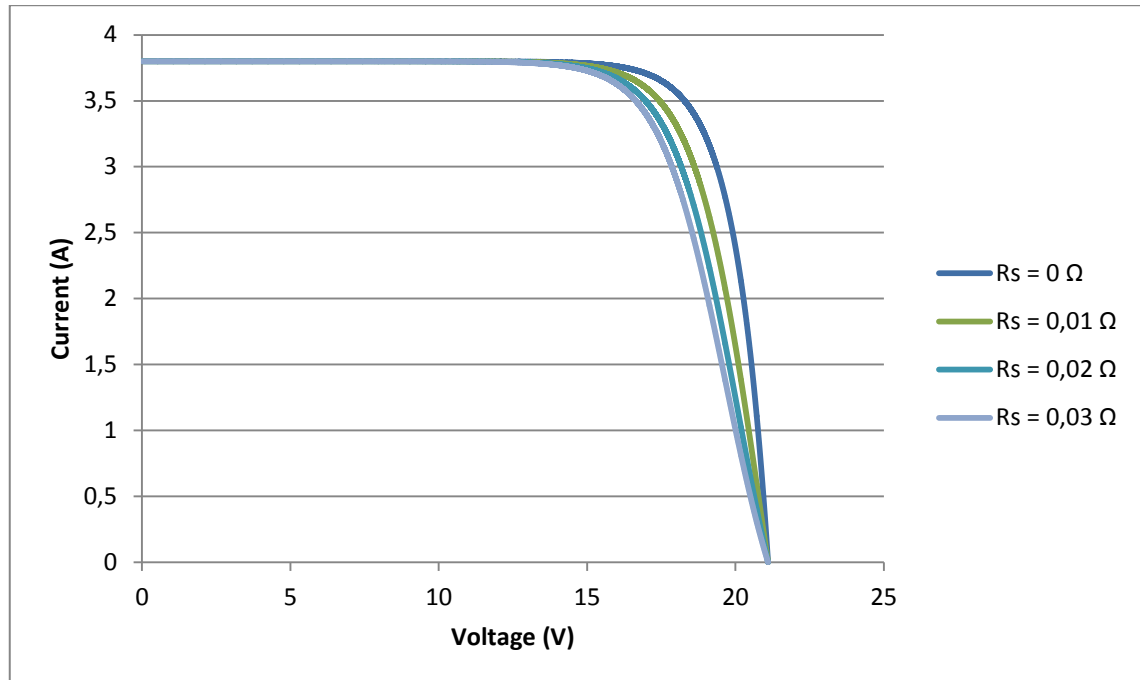


*Figure 22. I-V characteristic as a function of series resistance*

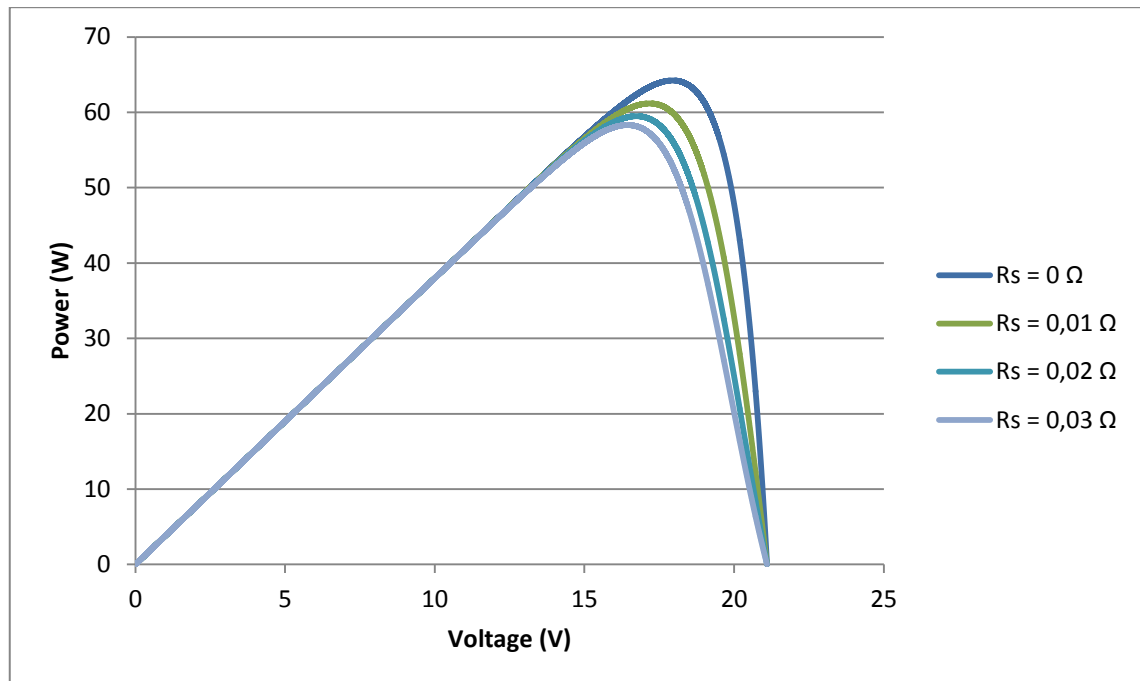


*Figure 23. P-V characteristic as a function of series resistance*

Photovoltaic solar panels are interconnected in series to form arrays / strings which in turn are connected in parallel. Solar panels similar electrical characteristics are grouped into strings. Each string is composed of  $N$  series-connected photovoltaic panels.

The (Fig.24) and (Fig.25) are providing information on associations in series. The voltage resulting from the panel increases proportionally to the number of cells, while the current is not affected.

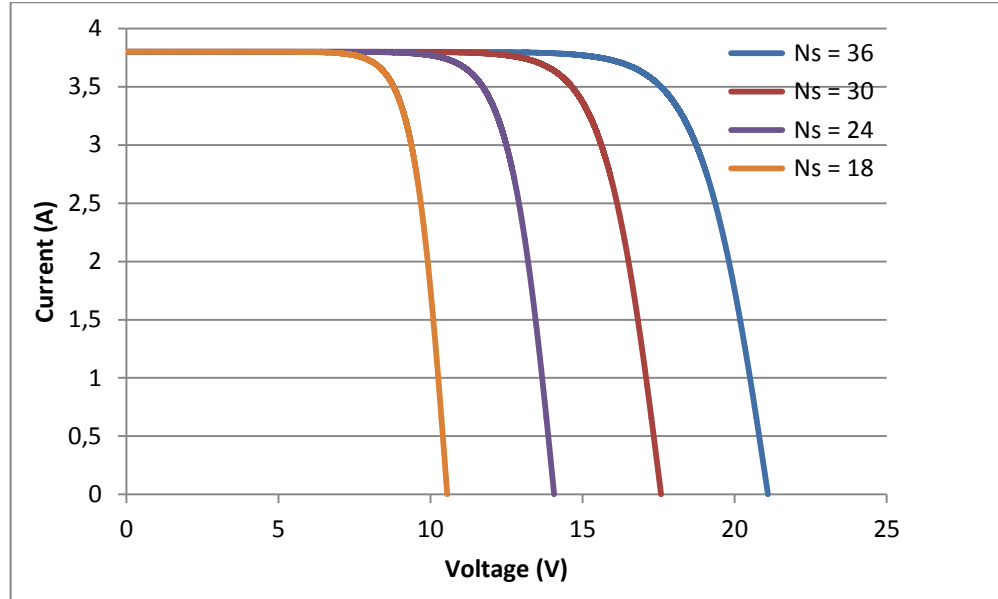


Figure 24. I-V characteristic as a function of the number of cells in series

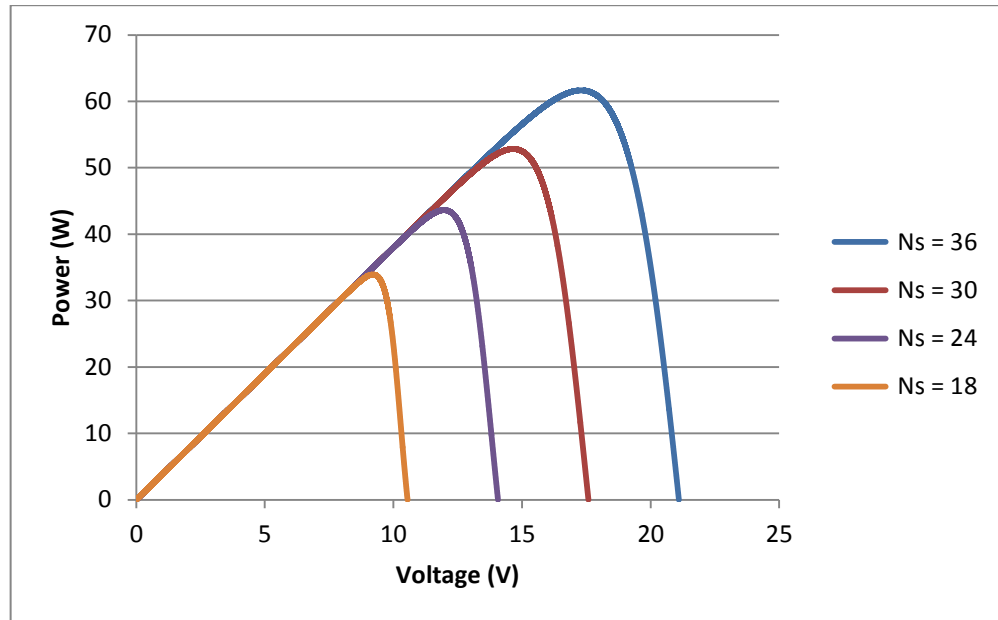


Figure 25. P-V characteristic as a function of the number of cells in series

The (Fig.26) and (Fig.27) are providing information on associations in parallel. The resulting intensity of the panel increases proportionally to the number of cells, while the voltage is not affected. It is observed that the power supplied by the panel is equal in both cases, since a proportional increase of the current or voltage.

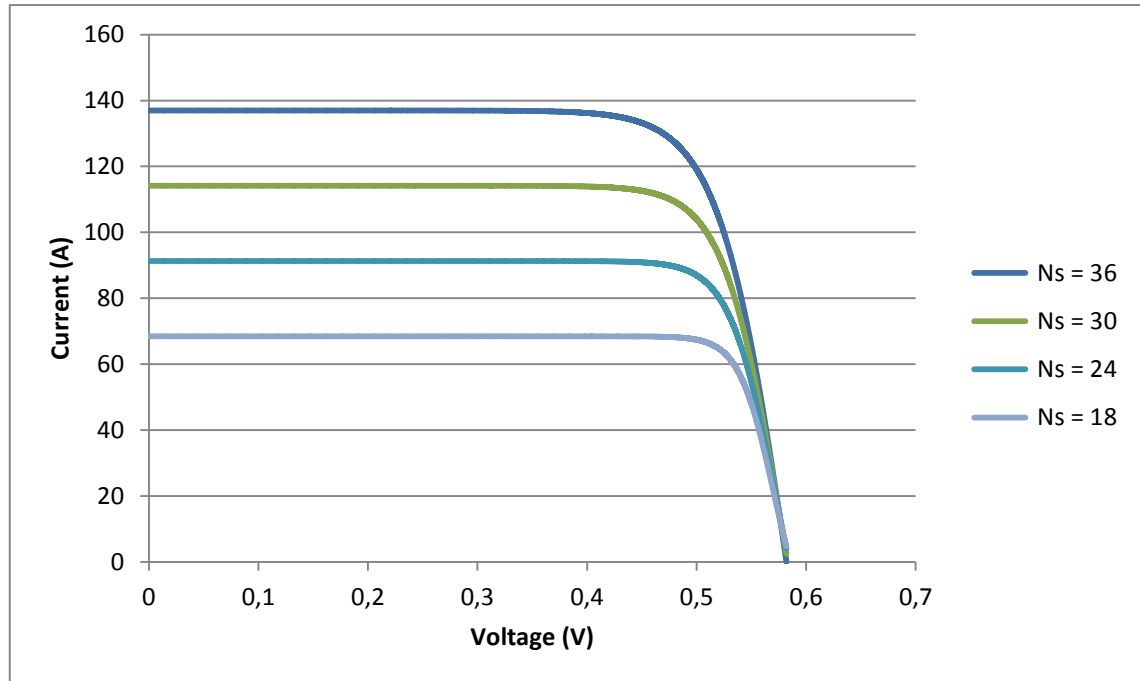


Figure 26. I-V characteristic as a function of the number of cells in parallel

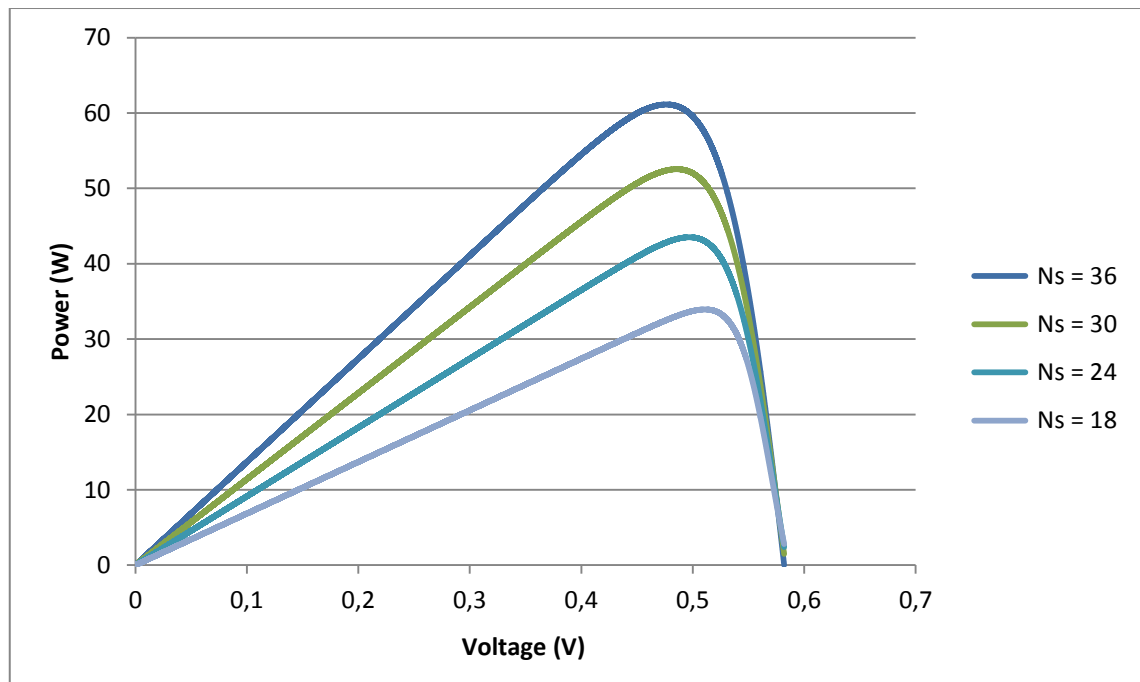


Figure 27. P-V characteristic as a function of the number of cells in parallel

# Chapter 4

## Software Design in LabVIEW

LabVIEW is a platform on which the programmer, using graphical language G and the virtual instrumentation, can simulate the behavior of equipment that are used in the area of electrical engineering.

The user will reduce costs, since LabVIEW can simulate hundreds of systems before to purchase the devices. LabVIEW offers a high-level graphic programming language and a friendly environment. The tasks can be executed much faster than in other languages, and it is quite easy for the programmer to create in a fast way a simulator easy to understand, for its intuitive graphical interface.

What concern us it is to build a simulator tool to simulate photovoltaic panels supplying, with the power supply controlled, an electric load. One of the objectives is to put the simulation of the PV panel close to the maximum power point, thus delivering to the load the highest possible quantity of energy. The MPP tracking is obtained by connecting a DC/DC converter between the solar panels and the load which could be the electric grid or a battery bank. In real situation the additional energy is stored in batteries and can be used later, when there is not enough sunlight and the PV panel cannot deliver enough energy to supply the grid.

### 4.1 - Obtaining I-V Curve

This section explains how to make the programming algorithm used to create the software. The algorithm is based on which is an example done in Matlab, whose script is presented below. Its parameters are the voltage at the panel terminals, radiation, and the operating temperature for a MX-60 panel (Fig.28). The user will introduce the climatic conditions, and the panel parameters provided by manufacturer, and the program will create the voltage sampling.

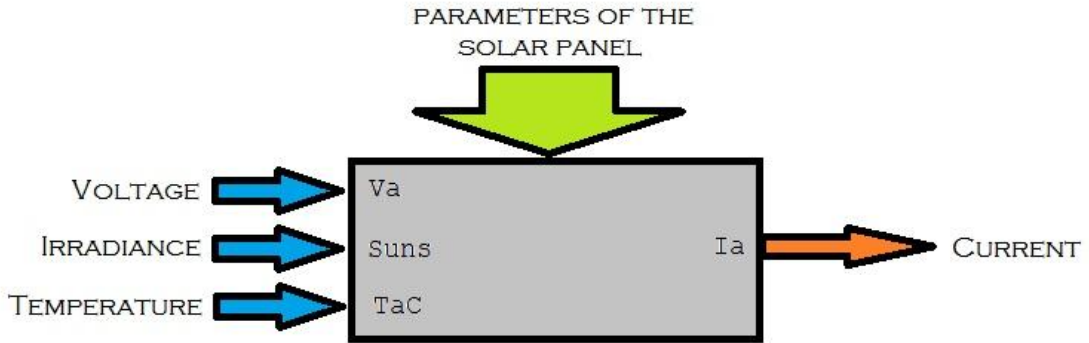


Figure 28. Inputs and outputs of the Matlab simulator

```

function Ia= solar(Va,Suns,TaC)
%For solar panel MSX-60
%Calculate the current through the voltage, irradiation and
temperature
Ia=solar(Va,G,T)=voltaje vector
%Ia,Va=current and voltaje vector
%G=number of Suns (1 sun=1000W/m^2)
%T=temperatura in Celsius
k=1.38e-23; % Boltzman's constant
q=1.60e-19; %electron charge
n=1.2; %diode quality factor
Vg=1.12; %Band voltage
Ns=36; %Number of series cell
T1=273+25;
Voc1=21.06/Ns; %Open circuit voltage per cell at T1
Icc1=3.80; %Short circuit current per cell at T1
T2=273+75;
Voc2=17.05/Ns; %%Open circuit voltage per cell at T2
Icc2=3.92; %Short circuit current per cell at T2
TaK=273+TaC; % To Kelvin
K0=(Icc2-Icc1) / (T2-T1);
I11=Icc1*Suns;
I1=I11+K0* (TaK-T1);
I01=Icc1/(exp(q*Voc1/(n*k*T1))-1); % Diode current
I0=I01*(TaK/T1).^(3/n).*exp(-q*Vg/(n*k).*((1./TaK)-(1/T1)));
Xv=I01*q/(n*k*T1)*exp(q*Voc1/(n*k*T1));
dVdI_Voc=-1.15/Ns/2; % Manufacter information
Rs=-dVdI_Voc-1/Xv; %series resistance per cell
Vt_Ta=n*k*TaK/q; % vt=AkT/q
Vc=Va/Ns;
Ia=zeros(size(Vc));

```

```
%Newton's method
for j=1:5;
    Ia=Ia- (Il-Ia-I0.* (exp((Vc+Ia.*Rs)./Vt_Ta)-1))./(-1-
(I0.* (exp((Vc+Ia.*Rs)./Vt_Ta)-1)).*Rs./Vt_Ta);
End
```

---

```
V=[0:0.1:24];
%Voltage sampling
Ia=solar(V,1,25);
plot(Ia,'r-');
axis([0 250 0 5]);
xlabel('Voltage');
ylabel('Current');
hold on;
```

**(For the understanding of this section is recommended the view of the annex 1.)**

Through the software created in LabVIEW user can also enter panel parameters as variables through a series of controls, in addition to irradiation and temperature of operation.

Once the mathematical model takes all the input parameters is performed within the SubVI 1 (fig.29) the calculation of  $I_L$ ,  $Rs$  and  $I_0$  with the equations (3.5), (3.6), (3.7), (3.8), (3.9), (3.10), (3.11) to arrive at this formula where we have just as unknown output current ( $I$ ), for a sampling of voltages created by a loop.

$$I = I_L - I_0 \left( e^{\frac{q(V+Rs \cdot I)}{n \cdot K \cdot T}} - 1 \right) \quad (4.1)$$

We can see that this equation is not linear due to the characteristic equation of the diode. So for the resolution is used Newton's method, with successive iterations to be performed until the method has converged sufficiently.

$$f'(X_n) = \frac{f(X_n)}{X_n - X_{n+1}} \quad (4.2)$$

If we had used two diodes in the electrical model approximation, this equation will be more complicated. The resolution of the formula will give us an array of intensities depending on the array created from 0 volts to the maximum open circuit voltage allowed by the panel.

The two arrays enter the SubVI 2 (Fig.30) to have the same number of elements and their values end up in court with the X axis, since we only care what happens in the first quadrant. You also get the maximum voltage ( $Voc$ ), the maximum current ( $Isc$ ), and create the scatter plot we created the IV curve. Within this SubVI also multiply matrices and voltage to find another chart that indicates the power that can be developed based on the panel voltage, determining the point of maximum power and the voltage and intensity where this occurs.

The SubVI 3 (Fig 31) takes the data taken from above to calculate the fill factor of the panel, with the equation (3.16).

Finally, the SubVI 4 (Fig.32) calculates the efficiency of the panel according to maximum power, irradiation, and a defined area, with the equation (3.17).

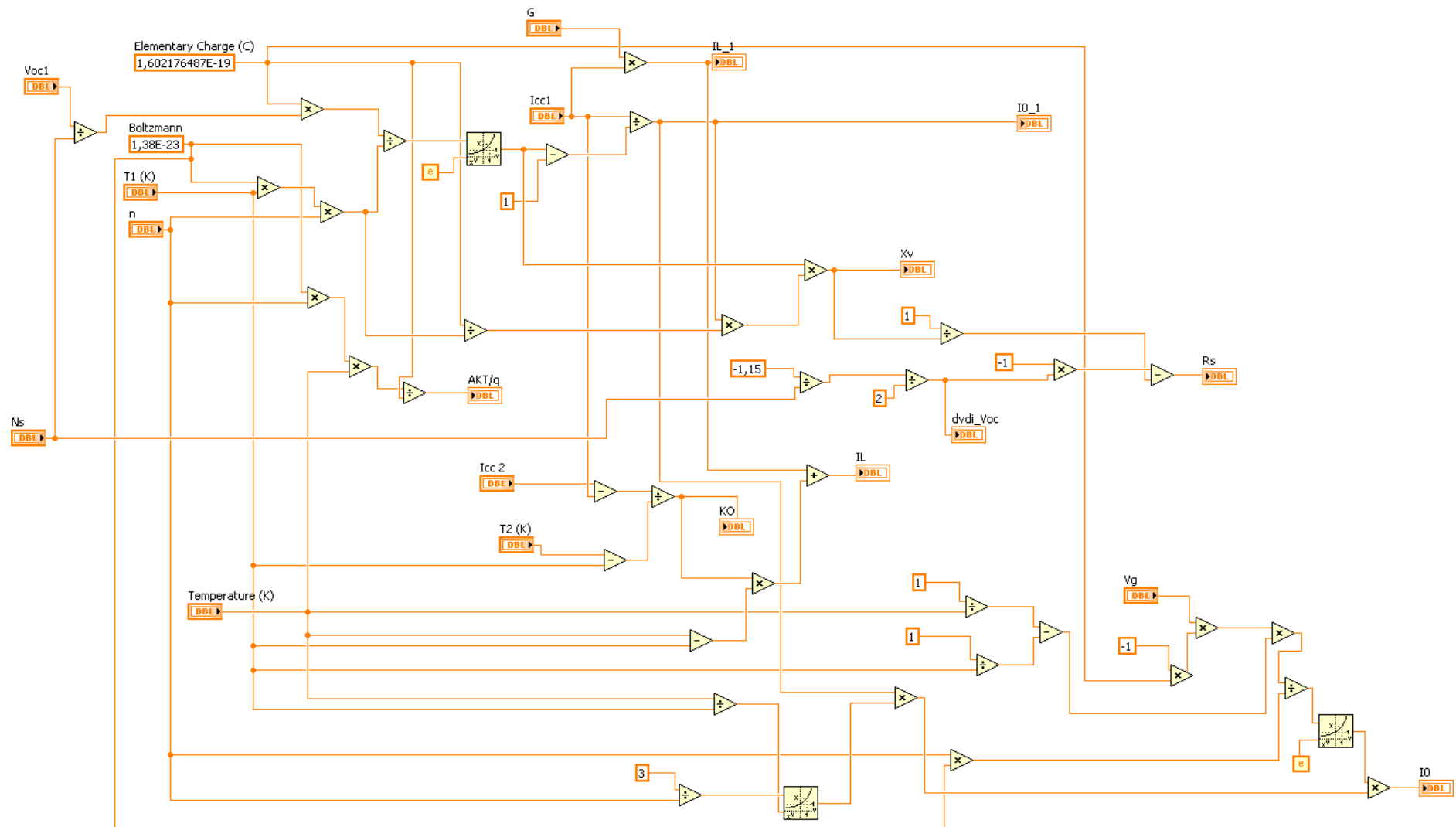


Figure 29. SubVI 1

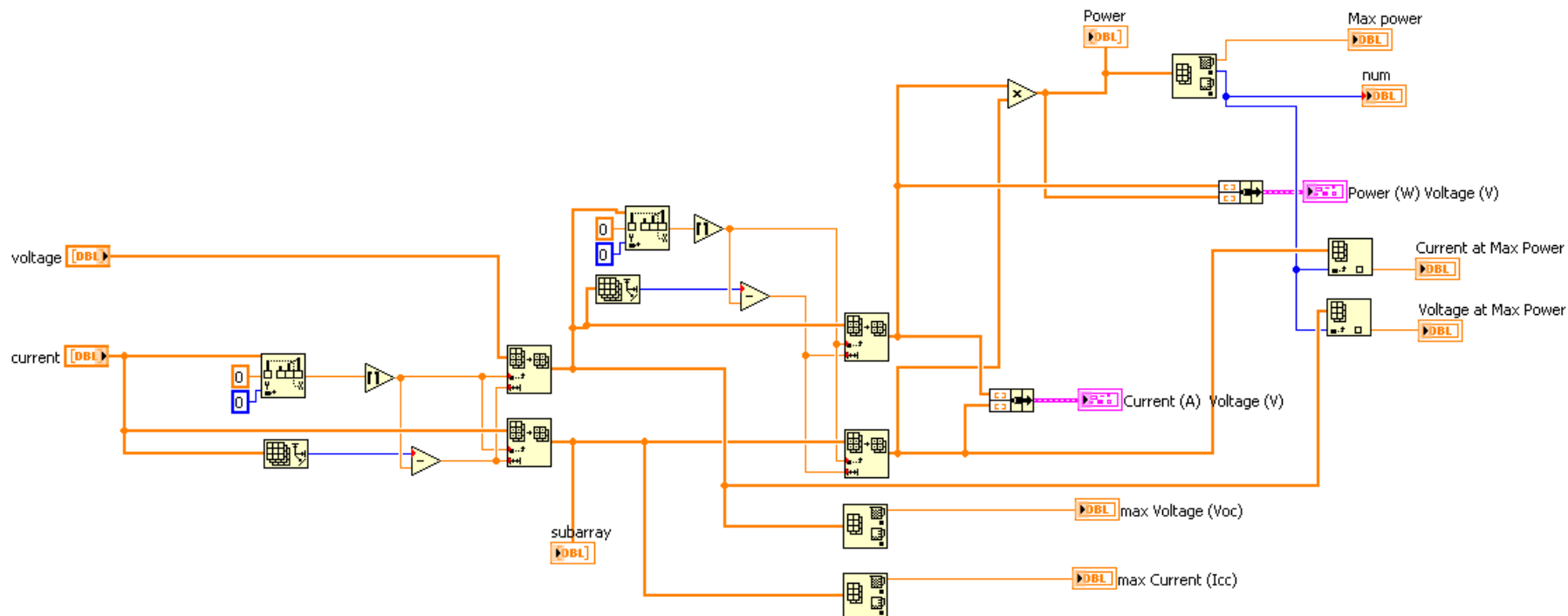


Figure 30. SubVI 2

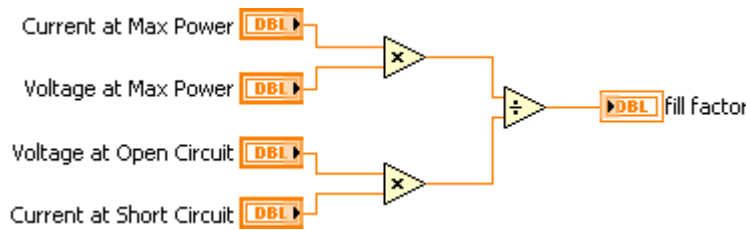


Figure 31. SubVI 3

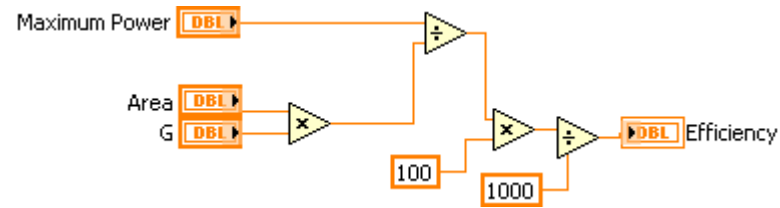


Figure 32. SubVI 4

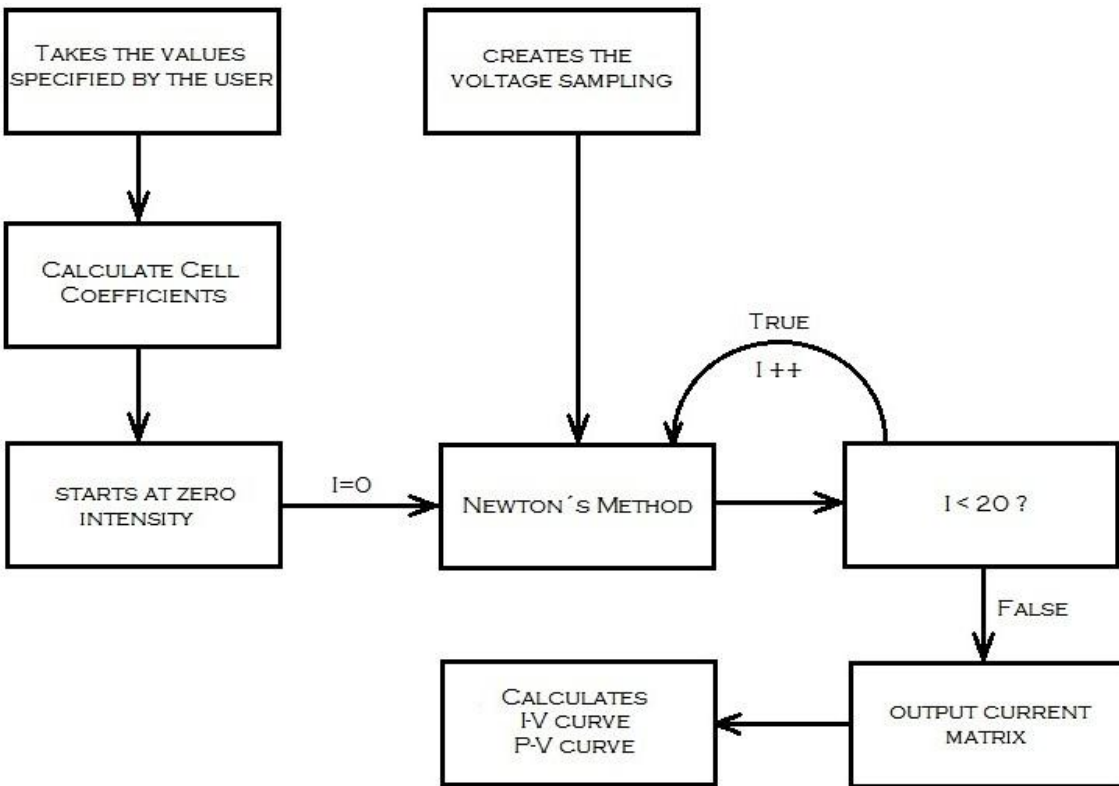


Figure 33. Algorithm used to obtain the IV curve

It is found that for the MX-60 panel, from the second iteration the intensity value does not vary more. However, as caution the number of iterations is 20, in case if it takes longer to reach convergence.

Apart from the creation of the curves, they were created three conditional structures associated with their corresponding switches, that are disable by default.

The first is to have direct control of the series resistance, although this depends on the temperature, so that the user could see the changes in the curve if this increases or decreases.

The second is created if the user wants to change the number of cells in series of the panel, if is already determined the number of cells ( $N_s$ ) given by the manufacturer. The third is another control to change the number of cells in parallel.

## 4.2 - Power Supply

The power supply is a vital part of the project, because it will be responsible for generating the voltage and current of the simulated panel. This section attempts to explain its functioning. The source will mimic the IV curve done by the algorithm and will simulate the photovoltaic panel as close as possible to the reality.

The programmable power supply allows controlling and maintaining constant the output voltage or output current of the load to which it is connected.

When the source operates in continuous current mode will give a constant current to the load at different voltages, which will be determined by the load connected to the source, according to Ohm's law  $V = I \cdot R$ . (Fig 34)

On the other hand when acting in the continuous voltage mode will give a constant voltage to the load at different intensities, which will be determined similarly by the load. (Fig.34)

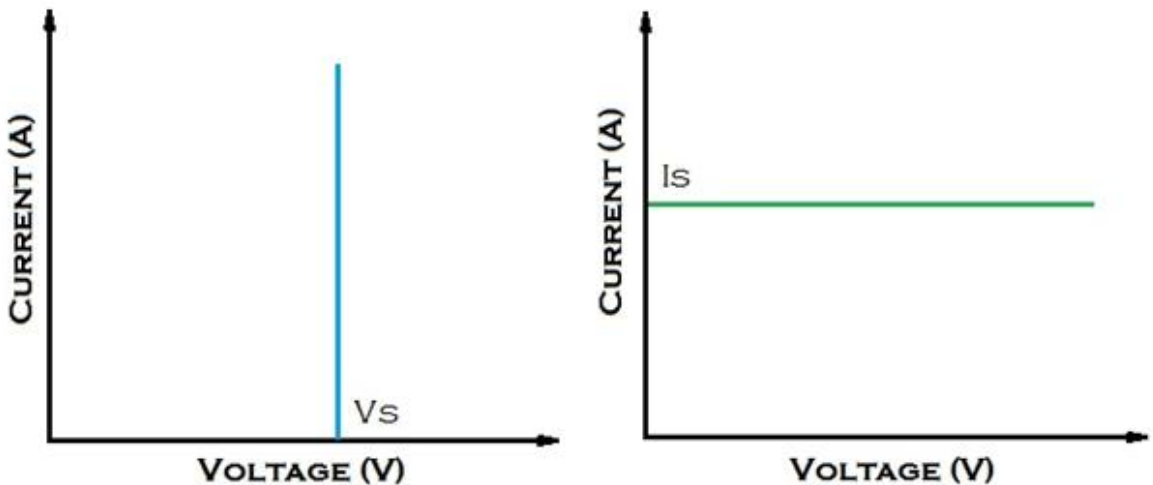


Figure 34. Output of a constant-voltage (left) and constant-current (right) supply

The point where the power switch from one mode to another depends on the load connected to it, in addition to the maximum current limit determined by the user.

When the load requires a greater amount of current than the limit set by the user, then the source will change to the constant current mode.

The resistance  $R_c$  is the critical resistance that determines the operating mode where the source gives the maximum power. (Fig.35)

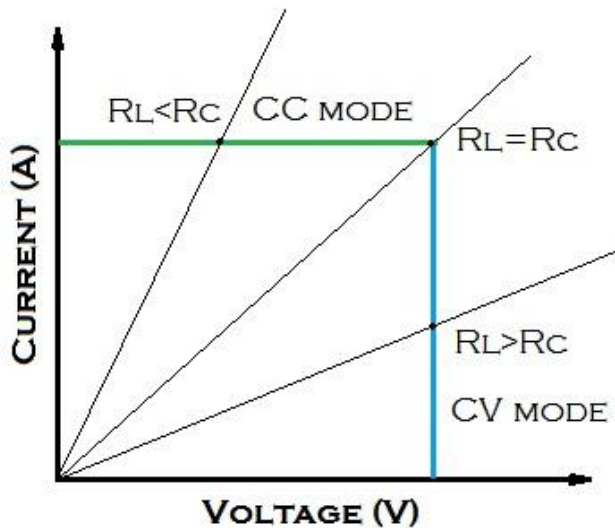
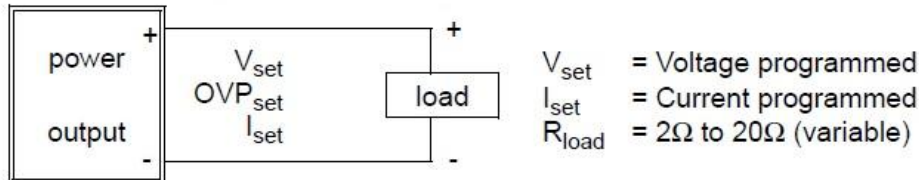


Figure 35. Output characteristic of a constant-voltage/constant-current supply.

Below is a numerical example taken from the user manual of the power supply used, where you can see clearly what was explained above.

Example for a variable load resistance:



Required: The  $V_{\text{set}}$  and  $I_{\text{set}}$  parameter have been coupled for the selected output channel.

- $I_{\text{Set}} = 1\text{A}$  Programmed current becomes 1A.
- $V_{\text{set}} = 8\text{V}$  Programmed voltage becomes 8V.

The crossover point resistance  $R_c = V_{\text{set}} / I_{\text{set}} = 8\Omega$ .

- If  $R_{\text{load}}$  increases from 8Ω to 16Ω, then  $R_{\text{load}} > R_c$ , so the output channel goes into the CV mode (refer to figure 5.5.7). This means that  $V_{\text{load}} = 8\text{V}$  and  $I_{\text{load}}$  becomes  $8\text{V}/16\Omega = 0.5\text{A}$ .
- If  $R_{\text{load}}$  decreases from 8Ω to 4Ω, then  $R_{\text{load}} < R_c$ , so the output channel goes into the CC mode (refer to figure 5.5.7). This means that  $I_{\text{load}} = 1\text{A}$  and  $V_{\text{load}}$  becomes  $1\text{A} \times 4\Omega = 4\text{V}$ .

The source with which they were tested in the laboratory is a Philips-Fluke PM2832. (Fig.36)



Figure 36. Philips-Fluke PM2832 power supply

The main characteristics are:

- Dual output
- $V_{\text{max}}=60\text{V}$
- $I_{\text{max}}=2\text{A}$
- $P_{\text{max}}=120\text{W}$



Figure 37. Philips-Fluke PM2832 power supply detail

The problem with using this source is that we cannot simulate panels above open circuit voltage over 60 V, which is not going to be a big limitation since most of the photovoltaic panels on the market fall within this range. The panels with high power, will have higher  $V_{oc}$  like the SunPower E19/320 Solar panel, that have an open circuit voltage of 64.8V and develops an output of 320 W. The supply will not support this range of powers.

But the greater limitation will be by the short circuit current because the PV panel to simulate it may not exceed 2 A. In conclusion: only the PV panels with small powers can be simulated.

Because of this limitation is advisable to use another power source with maximum intensity values higher. This source is used because that is what was available in the laboratory; however the procedures to emulate the higher power panels are analogous to those performed.

In order to test the hardware, we are going to change the panel so far used for the analysis of the graphs, the msx60, because this one have a short circuit current of 3.8 A, but also will prove the MSX60 reducing the value of the irradiation from 1000W/m<sup>2</sup> to 100W/m<sup>2</sup>, thus, the current will fall and the simulation will be within the limits of the source. In Chapter 5, experimental results this will be shown.

The source is connected to a rheostat. The rheostat resistance will vary from short circuit to a 100 ohm resistor, which simulates an open circuit. Because of this you can check if the source mimics the curve created in LabVIEW, from  $V_{oc}$  to  $I_{sc}$ .

### 4.3 - Hardware Implementation

To control the power source with the voltage and current values given by the curve previously created, the algorithm that is used is explained below.

The method is to find the point of intersection between the curve and the line of resistance.

It creates a line from the origin to the measured output current. The line is equivalent to the resistor connected to the source ( $1/R$ ). The intersection between the line and the curve will be the working point; the algorithm is used to find this intersection, and change the supply voltage, with the new values obtained. This method works in all regions of the curve. Both the line of resistance as the curve will have a very high number of points for the two lines intersect at a particular point. (Fig.38)

If the resistance is higher the line will approach more to the open circuit point. In my case the line sweeps from 0 ohm in the  $I_{sc}$  point to the 100 ohms near the  $V_{oc}$  point. If the user wants to approach more to the  $V_{oc}$  point only have to increase the resistance. This is shown in figure 40.

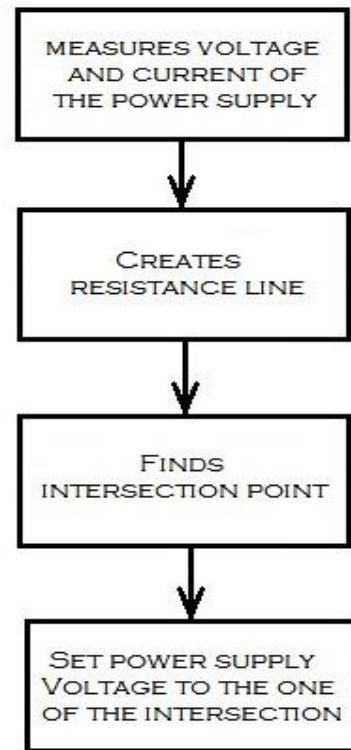


Figure 38. Algorithm used to set the supply

(For the understanding of this section is recommended the view of the annex 2.)

These were the steps taken:

- Find a LabVIEW driver for PM2832 source.
- Set the source to synchronize the communication port channel chosen GPIB with LabVIEW.
- Initialize the source, and set as 110% of the short-circuit current the initial intensity.
- Read the output current and voltage source, which depend on the load.
- Taking the above data to interpolate a straight  $I / V = 1 / R$  in the SubVI 5 (Fig. 39).
- Subtract the current array of the curve with the current array of the line, to find a point where they become zero.
- Find that point in the voltage array of the curve.
- Enter the voltage value of the intersection at the source of power.
- Repeat the process and graphically display the cutoff point.

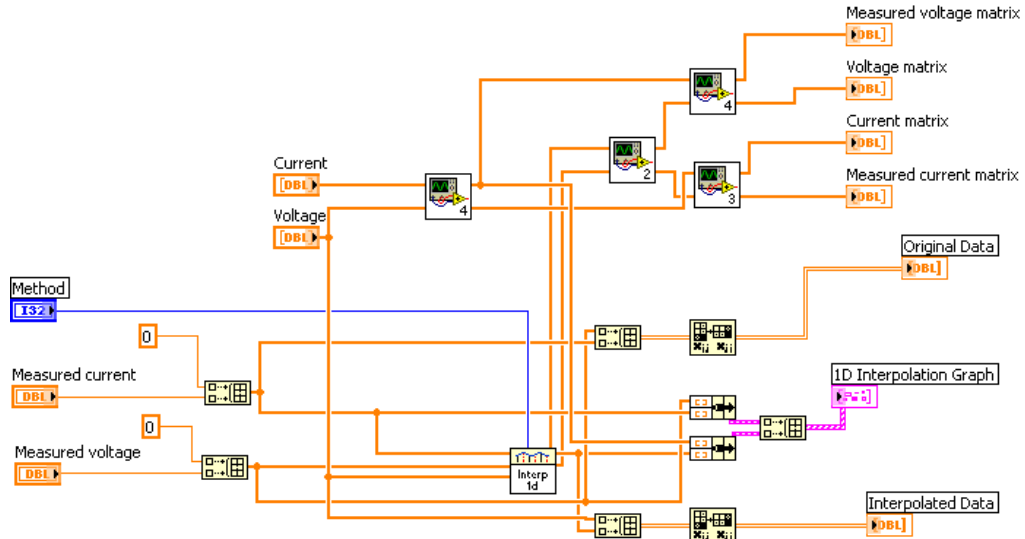


Figure 39. SubVI 5

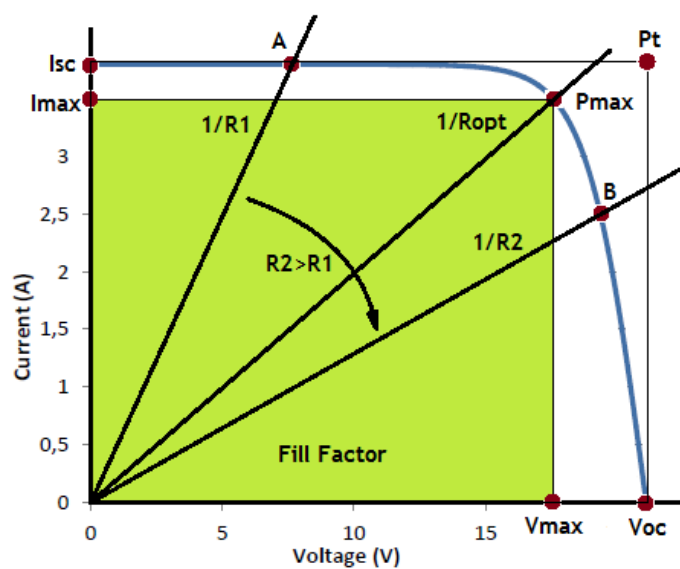


Figure 40. Resistance line

# Chapter 5

## Experimental Results

### 5.1 - Workplace and Switchgear Used



Much of the work performed and which required the use of switchgear for the hardware implementation and test of different photovoltaic panels has been developed in the laboratory I105 from the department of electrical and computer engineering of FEUP. The rest of the work was done on my home computer. Figure 41 shows from top to bottom the connection scheme of the elements involved.

First, the **computer** will be responsible for sending the signals through the LabVIEW Plug and Play Instrument Driver of the power supply to remotely control this one. The connection with this will be done through a GPIB Controller for Hi-Speed USB. The connection **GPIB-USB-HS** (IEEE 488.2) it is from National Instruments, and you can download the drivers at his website [22]. The computer and the power supply will have to be configured with the same GPIB communication channel, which was quite tricky. You must perform the following steps:

- 1) In LabVIEW: Tools - Measurement and automation explorer - My system - Devices and Interfaces - GPIB0. Then change the primary address to a number between 1 and 30.
- 2) In the Philips/Fluke power supply: press the AUX as many times as necessary to display ADDRESS, and enter the number chosen in LabVIEW.

Figure 41. Connection Scheme

The power supply **Philips/Fluke PM 2832** launch date was from January of 1997 so it is quite old, now is discontinued, but was very useful to test the concept. Finally **rheostat of 100 ohms** is connected to the power supply, to have the variable resistor. The figure 42 shows a general view of the workplace and the switchgear.

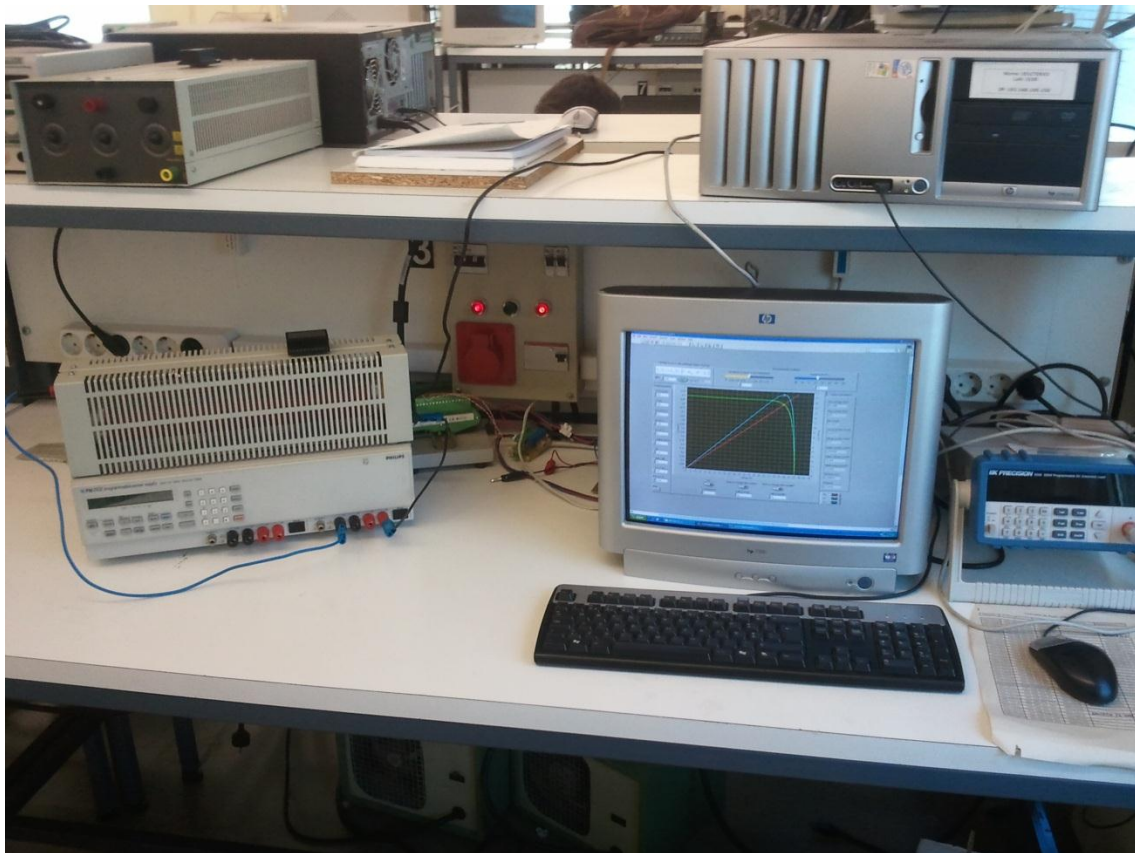


Figure 42. Workplace

## 5.2 - User Guide

The user could download the program at [http://paginas.fe.up.pt/~ext11140/?page\\_id=23](http://paginas.fe.up.pt/~ext11140/?page_id=23) called “LabVIEW Simulator.rar”, inside, the user will see two programs, and a folder called “SubVI” with the files necessary for the operation of these. Also there are the National Instruments Drivers for the Philips/Fluke power supply. This is the folder where the drivers must be introduced: C:\Program Files (x86)\National Instruments\LabVIEW 2011\instr.lib.

The user could use two programs, one that support the hardware “With Hardware.vi”, and the other one that it is develop without hardware “Without Hardware.vi”. If the user don’t have the hardware needed, or he only wants to view the characteristic curve of a panel at the market, he has to use the one called “Without hardware.VI”. The advantages of this program is that don’t have limitations in order to emulate any type of panels, since the program it is only mathematical based, it don’t have the limitations of the power supply characteristics. However, the main objective of the thesis is to create a simulator through the power supply, so from here we analyze the program with hardware.

Below it is explained how to understand the LabVIEW front panel of the simulator (Fig. 43). The interface without hardware is analogous to this, so is explained the most complex.

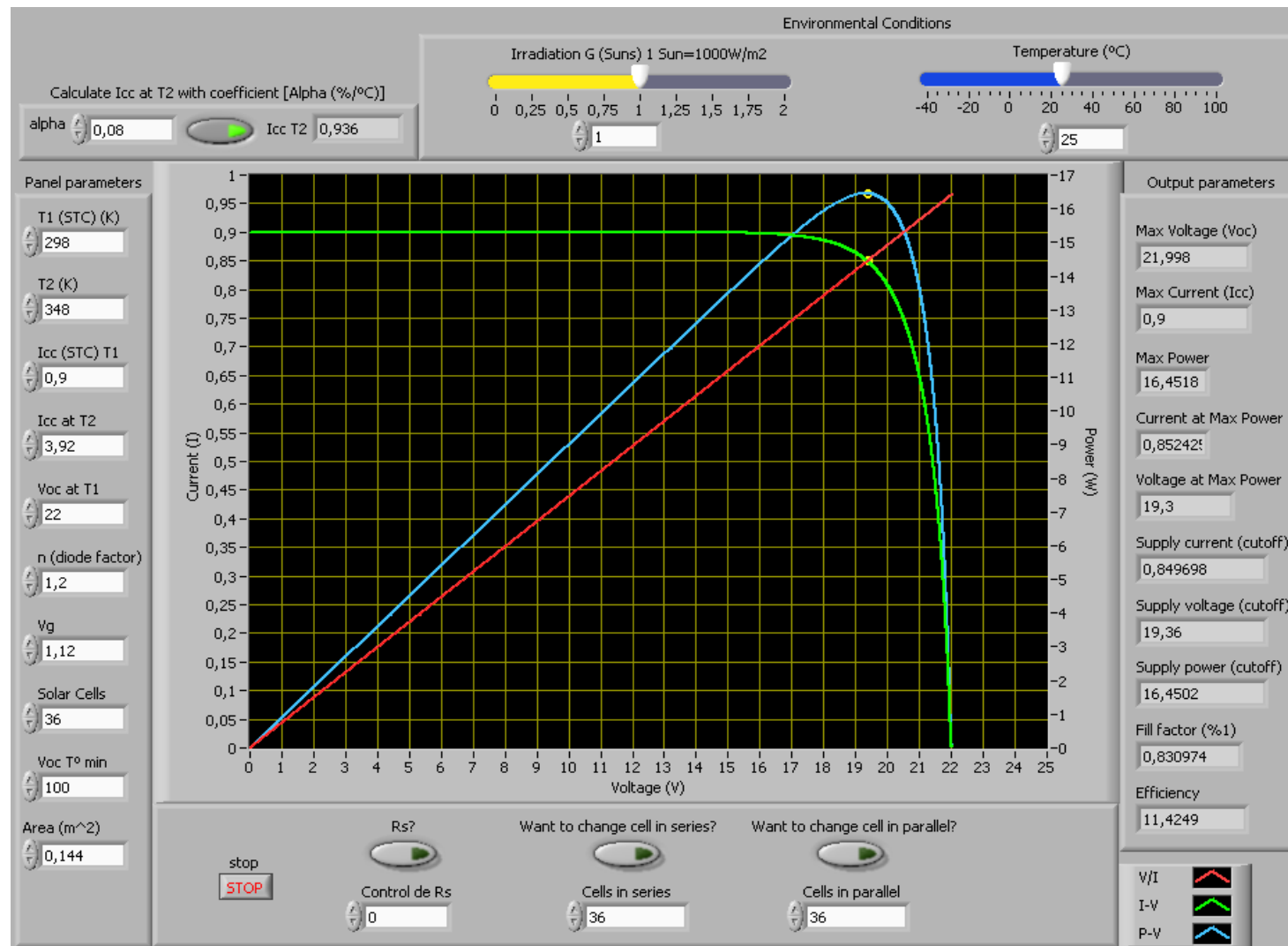


Figure 43. LabVIEW Front Panel of WITH HARDWARE.VI

The front panel of LabVIEW it is a graphical and intuitive interface that shows the characteristic curve of the panel simulated and his operating point. Also shows the power curve with his corresponding point.

The left column is reserved for the panel parameters, where the user will introduce all the characteristic parameters, which are easy to find out in the manufacturer's website. The parameters of T1, T2 there would almost never be changed, because they are usually defined by the manufacturer, and the Voc T°min almost never change the functioning of the cell, so rarely it's going to be changed.

At the top left the user could calculate the Isc at temperature 2, which is able by default. The variations of the short circuit current due to the temperature of the panel usually are given by the manufacturer with a coefficient "alpha" (%/°C). So if this alpha is changed, the program automatically calculates the new Isc at T2.

At the top right there are the controls of the operating temperature of the panel, and the solar irradiation, which are by default in the STC conditions (25°C, 1000W/m<sup>2</sup>).

Just below the graph it's the STOP bottom that ends the program; also there is a direct control of the series resistance of the panel, and another two controls, to change the number of cells in series or parallel. All three are disable by default. It's important, that if the user want to change the number of cells, it have to be the original number of cells in series of the panel to simulate. The right side of the graph is for the column of the output parameters. These indicators depend on the variables chosen. The values called with (cutoff) are the ones that correspond to the values of the supply. So if the user wants to simulate the maximum power allowed by the panel under the environmental conditions has to modify the resistance until the value of Max Power it's the same as the value of Supply Power (cutoff). Finally at the bottom right is the legend of the chart.

These are the steps required to use the simulator:

- Connect the supply to the computer via the GPIB port
- Connect the supply to the resistor
- Open WITH HARDWARE.vi
- Enter the desired input parameters (Panel parameters and environment conditions)
- Press RUN
- Vary the resistance to find the desired operating point
- Press STOP to end

The advantages of this program is that change in real time. You don't have to STOP the program to change the input parameters, or the resistance, the curve will change according to changes and the program looks for the new operating point quite quickly.

### 5.3 - Test Panels

In this chapter are tested some commercial panels, to see how reliable is the simulator developed. The panels are compared with the I-V curves, and the characteristics provided by the manufacturer. At the end of this section, they are some conclusions of the tests done.

The panels chosen are the following:

- Sharp Electronics Corporation NU-U208FC
- Solarex MSX10
- Solarex MSX60

For testing the panels are necessary know the values of the diode quality factor and the band gap voltage of the different materials used in the cells (Table 1)

Cell Type	Diode quality factor (n)	Bandgap Voltage (Vg)
Mono-Silicon	1.026	1.11
Poly-Si	1.025	1.14
a-Si:H	1.8	1.65
a-Si:H tandem	3.3	2.9
a-Si:H triple	3.09	1.6
Cadmium telluride (CdTe)	1.5	1.49
Copper Indium Selenide (CIS)	1.5	1.48
Gallium arsenide (AsGa)	1.3	1.43

Table 1. Diode quality factor and band gap voltage

Another thing to keep in mind is that values of voltage and current given by the manufacturer are for the STC conditions, so for another temperatures or irradiance is more complicated to compare the simulator, however some manufacturers, for example Solarex, gives a graph of the behavior at different temperatures, and the manufacturer Sharp gives a chart of the behavior at different irradiance. They are chosen these panels in order to test all the possible variations of the simulator and check that it works correctly.

### 5.3.1 - Sharp Electronics Corporation. NU-U208FC [7]

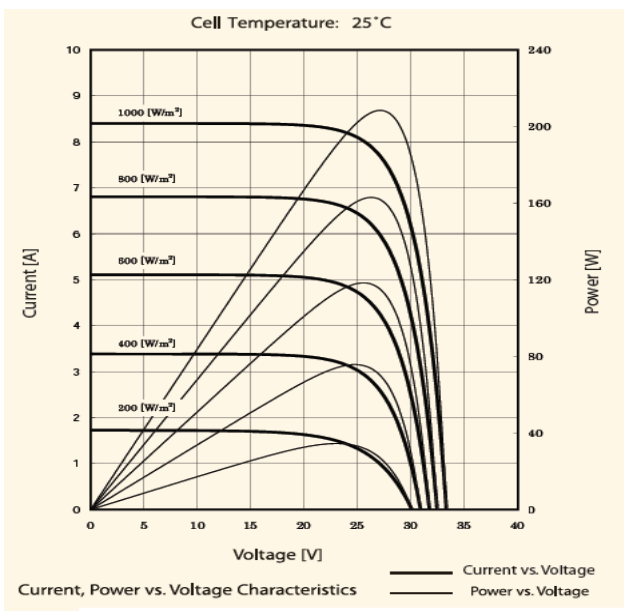


Figure 44. SHARP UN-U208FC from data-sheet [7]

At figure 44 we can see the curves corresponded to the UN-U208FC SHARP panel from the datasheet. This panel exceeds the limits of current of the power supply, so the simulation of the curves is done with the program without hardware. As we can see, the simulator (fig. 45) conforms quite well to reality, since the model given by the manufacturer notes at 25°C and 1000W/m<sup>2</sup> the maximum power in 208W, while our simulator indicates a maximum power of 206.05 W for a diode quality factor of 1.026, and band gap of 1.11 V the values for monocrystalline silicon panels.

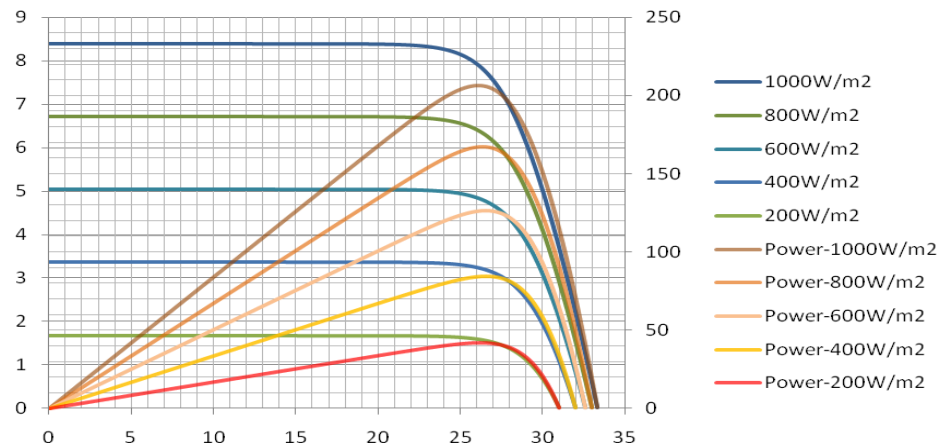


Figure 45. SHARP UN-U208FC for different irradiance from simulator

The simulator plots the I-V and P-V curve at different irradiances quite similar than does in the datasheet, with a slight error. At table 2 are shown the percentage deviations of the electric parameters at maximum power and the efficiency calculated with the area.

Parameters	Manufacturer Data	Simulator Results	Percentage Deviation
V <sub>mp</sub> (V)	27.4	26.058	5.102 %
I <sub>mp</sub> (A)	7.6	7.907	4.039 %
P <sub>max</sub> (W)	208	206.055	-0.936 %
Efficiency (%)	14	13.9038	-0.6872 %

Table 2. Experimental Results for SHARP UN-U208FC

### 5.3.2 - Solarex. MSX10 [8]

This panel meets all requirements with the power supply. The rheostat has been changed, moving the resistance line until meet the intersection point with the I-V curve that provides the greatest power. So the supply is set up with the theoretical max power of the simulated panel.

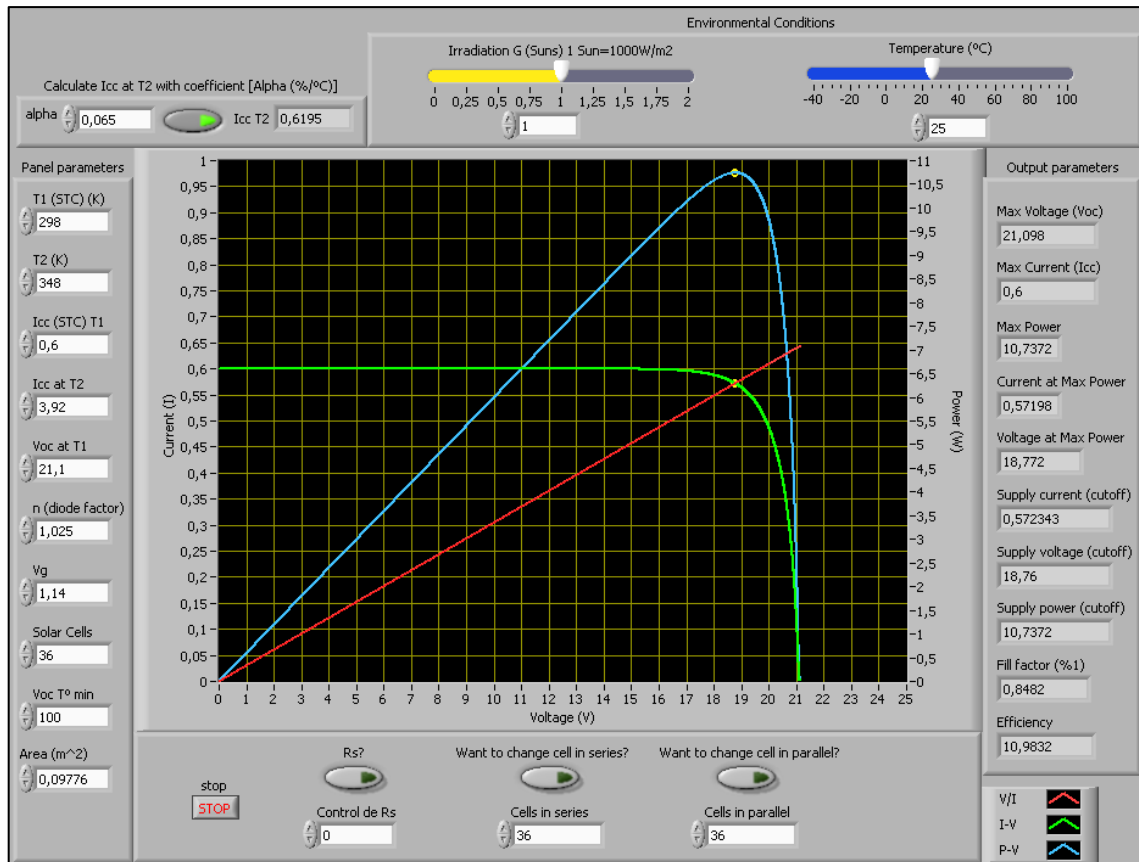


Figure 46. Solarex MSX-10 for STC from simulator

Parameters	Manufacturer Data	Simulator Results	Percentage Deviation
Vmp (V)	17.1	18.76	9.707 %
Imp (A)	0.58	0.572	-1.38 %
Pmax (W)	10	10.7372	7.372 %
Efficiency (%)	11	10.9832	-0.1527 %

Table 3. Experimental Results for Solarex MSX10

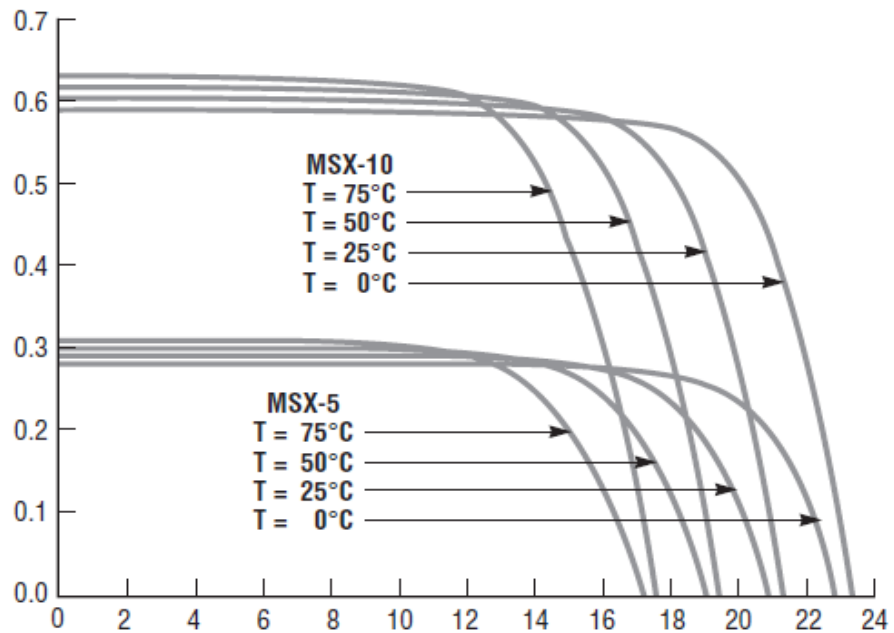


Figure 47. Solarex MSX-10 for different temperatures from datasheet [8]

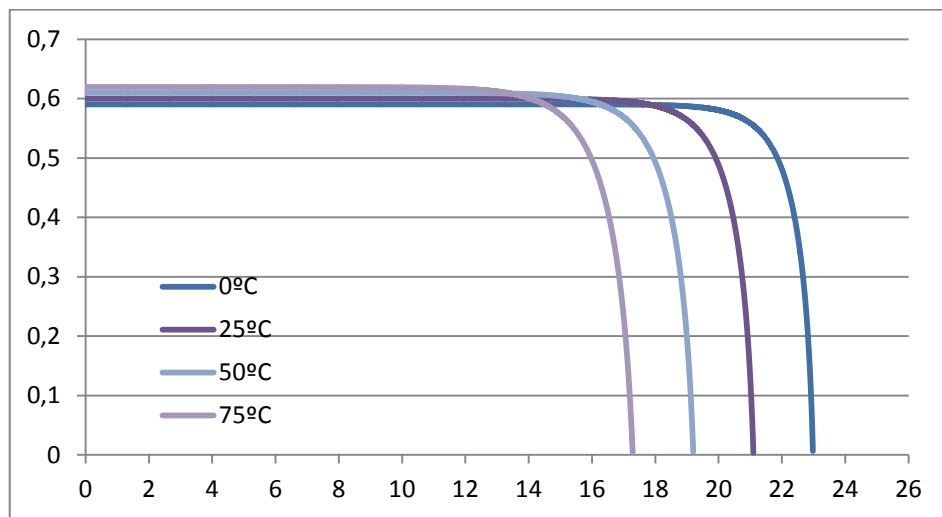


Figure 48. Solarex MSX-10 for different temperatures from simulator

### 5.3.3 - Solarex. MSX60 [9]

Since this panel has a short circuit current more than 2A we can't simulate with the supply, but by decreasing the radiation of  $1000\text{W/m}^2$  to, for example,  $100\text{W/m}^2$  simulated panel will decrease his short circuit current and it is shown that works perfectly within their ranks. Also the comparative analysis is done through the without hardware simulator as in the previous case with the Sharp panel, to determine its precision.

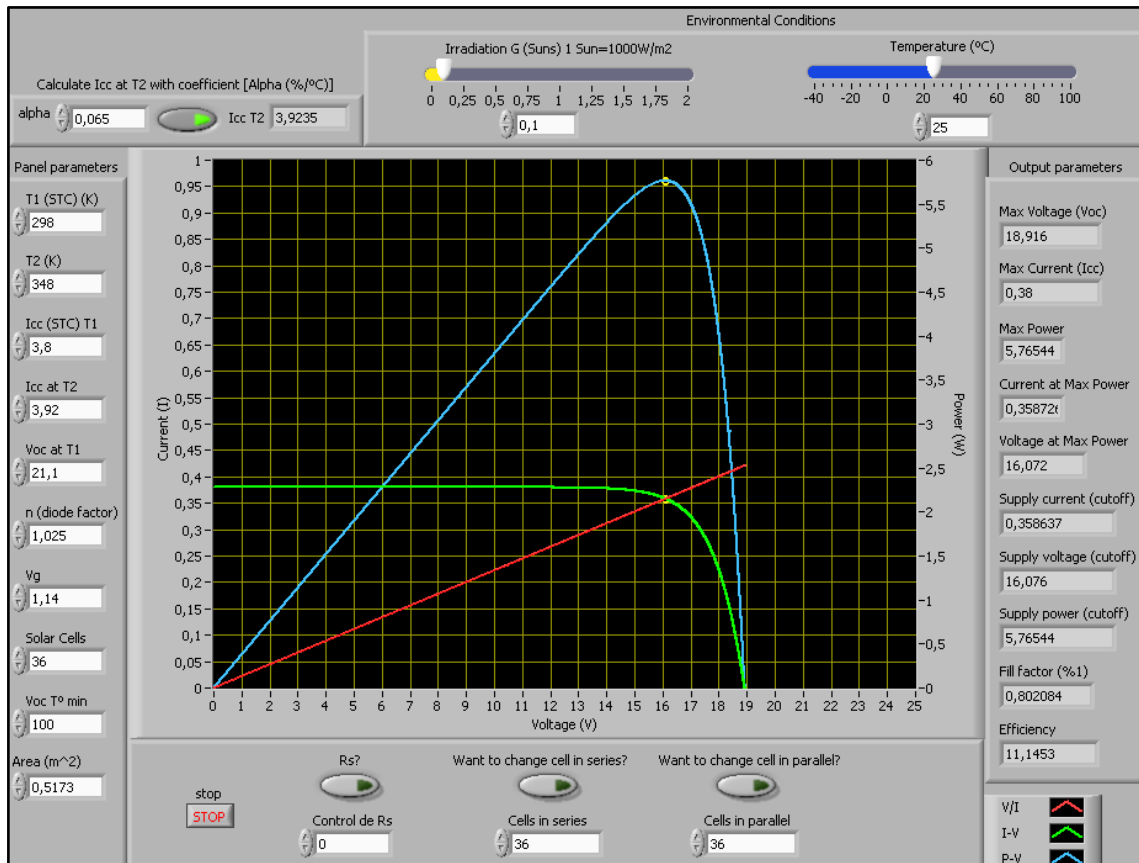


Figure 49. Solarex MSX-60 for 100W/m<sup>2</sup> from simulator

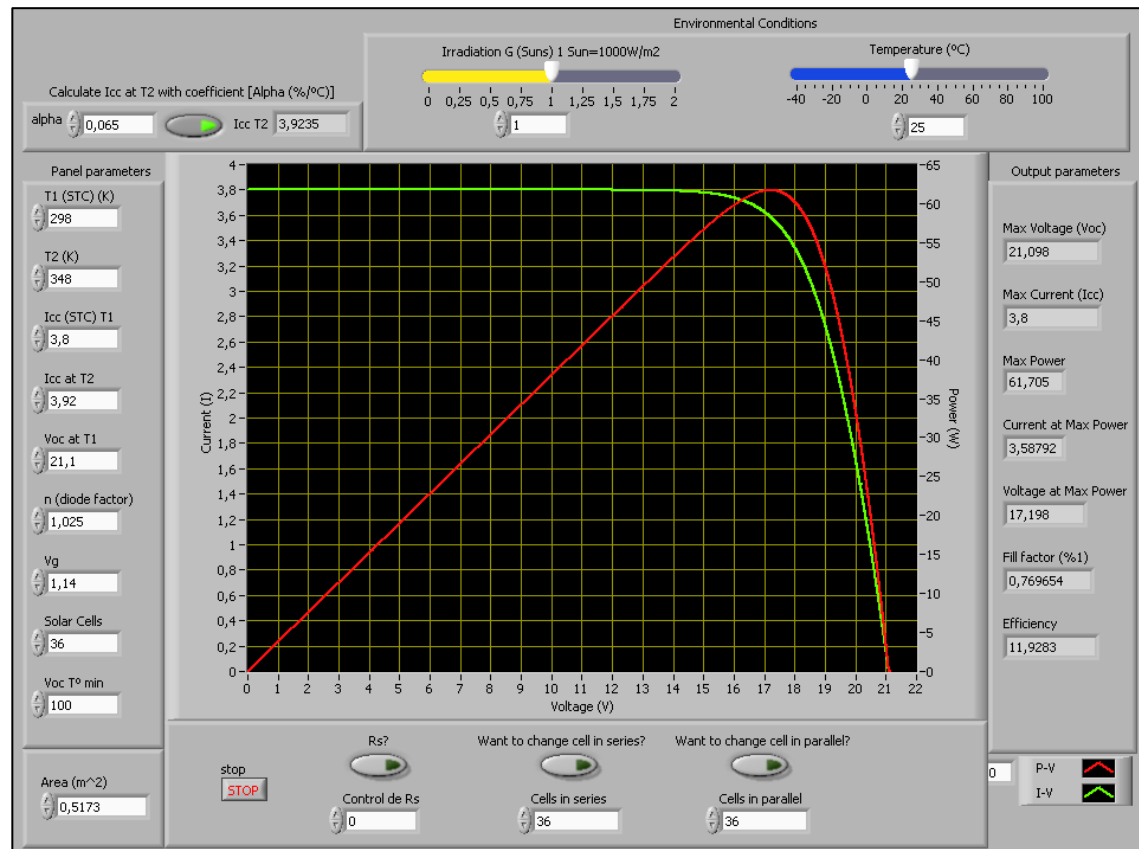


Figure 50. Solarex MSX-60 for STC from simulator

Parameters	Manufacturer Data	Simulator Results	Percentage Deviation
Vmp (V)	17.1	17.19	0.526 %
Imp (A)	3.5	3.58	2.2857 %
Pmax (W)	60	61.7	2.84 %
Efficiency (%)	12	11.928	-0.6 %

Table 4. Experimental results for Solarex MSX-60

## 5.4 - Testing conclusions

There have been done a series of trials to test the proper operation of the simulator. Logically, when irradiation increases and the operating temperature decreases, the maximum power that the panel can deliver to the load is greater.

Moreover the accuracy of the panel output characteristics differ little from reality. We analyzed the behavior of the panel at the knee of the curve, the most interesting place since it is where the maximum power occurs. It has been shown that the errors obtained are of approximately 5% of the expected value. But these errors are very different between tests, so do not follow a particular pattern.

Errors can come as a result of simplification of the electric model of the panel, since it is not taken into account the parallel resistance of the leakage currents. Furthermore, it has been taken that the values of the series resistance of each panel are the same and this is not true. For all three panels are taken the series resistance of MSX60 Solarex panel, giving rise to greater errors with it. Also this explains the error is so low in this panel. The reason for not changing the series resistance is because it is a piece of information with difficult access, which cannot be found in a simplified datasheet as those found online. However, if the user has the data of the value of the series resistance of the panel to emulate, he has only to activate the Boolean located at the bottom left of the simulator and input the data there.

In conclusion the simulator developed can emulate via a power supply with acceptable errors at least all the panels up to 20W, leaving the panels with higher power a software simulation, which does not allow the testing of photovoltaic equipment.

# **Chapter 6**

## **Conclusions and Future Research Areas**

### **6.1 - Conclusions**

The growing demand and implementation of photovoltaic power generation systems required to investigate and develop emulators that allow for testing and improving these systems. The design of photovoltaic systems is complicated due to the variability of weather conditions. In this work has been developed a photovoltaic emulator able to test photovoltaic inverters and MPPT algorithms in conditions close to real.

Currently there are equipment that can perform these testing, but are based on actual solar panels that are illuminated by the sun or artificial light source, the problem with this type of emulators is directly dependent on climatic conditions in the time of testing, in addition to poor performance and they cannot get high power from a single panel.

The software developed in LabVIEW to control a power source for this has the characteristics of a photovoltaic panel. Given a user-specified load the emulator displays an output voltage and current for the type of panel to be simulated, and the temperature and irradiation conditions desired. This will test and improve the photovoltaic system components such as inverters or banks of batteries.

The software can be used to analyze the functioning of photovoltaic module and helps to do a system design and get the performance of the available modules on the market without the need of purchasing them for tests. Due to its good precision can be simulated several types of panels.

## 6.2 - Research and Improvements Areas

One way to improve the simulator will be implementing a data acquisition system and integrate it in the software. A temperature sensor, a light intensity meter, and a conventional solar panel can vary the temperature and irradiance of the simulator over a day, to determine the efficiency of longer-term panel.

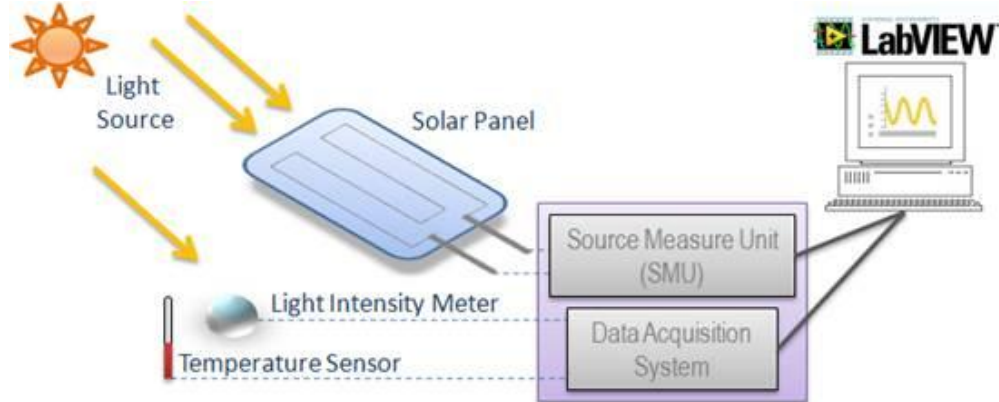


Figure 51. Example of a Photovoltaic Test System [10]

It can be add a database with the parameters of many panels, so that the user does not have to know the characteristics of each panel to simulate, you can simply look for the panel within a list, and LabVIEW are responsible for enter the relevant data.

Another way to continue the work will be to introduce a number of parameters to make the panel work in terms of a time and place. For example, determining a month of the year, time of day and location for placement of the panel, gives a result dependent on the actual conditions of the environment. It could also take into account the effect produced by the partial shading, because a photovoltaic generation system with X panels have a level of irradiation heterogeneous, especially at dawn or sunset or sporadically over a cloud.

It could also investigate a custom power supply for the simulator to be able to simulate most of the solar panels, reducing hardware costs.

# References

- [1] Ren21. Renewables 2011 Global Status Report. 11 July 2011  
[http://www.ren21.net/Portals/97/documents/GSR/REN21\\_GSR2011.pdf](http://www.ren21.net/Portals/97/documents/GSR/REN21_GSR2011.pdf)
- [2] Hawk Energy Solutions. Solar PV System Energy. 2010.  
<http://www.solar-pv-system.com/Solar-PV-System/Solar-PV-Energy.html>
- [3] Wikipedia. Band Gap. Last modified on 7 December 2011  
[http://en.wikipedia.org/wiki/Band\\_gap](http://en.wikipedia.org/wiki/Band_gap)
- [4] Wikipedia. Shockley-Queisser limit. Last modified on 28 January 2012  
[http://en.wikipedia.org/wiki/Shockley%20%93Queisser\\_limit](http://en.wikipedia.org/wiki/Shockley%20%93Queisser_limit)
- [5] Four Peaks Technology. Solar Efficiency Limits. 2010.  
[http://solarcellcentral.com/limits\\_page.html](http://solarcellcentral.com/limits_page.html)
- [6] National Renewable Energy Laboratory (NREL), Golden, CO. February 2012.  
<http://www.nrel.gov/ncpv/>
- [7] Sharp Electronics Corporation. NU-U208FC Solar Panel Datasheet. 2009  
[http://files.sharpusa.com/Downloads/Solar/Products/sol\\_dow\\_NUU208FC.pdf](http://files.sharpusa.com/Downloads/Solar/Products/sol_dow_NUU208FC.pdf)
- [8] Solarex. MSX5/MSX10 Solar Panel Datasheet. November 1998  
<http://www.deltastrumenti.it/misura/Datataker/MSX10.pdf>
- [9] Solarex. MSX60/MSX64 Solar Panel Datasheet. 1998.  
<http://www.californiasolarcenter.org/newssh/pdfs/Solarex-MSX64.pdf>
- [10]National Instruments Corporation. Tutorial I-V Characterization of Photovoltaic Cells Using PXI, February 2012. <http://zone.ni.com/devzone/cda/tut/p/id/7231>
- [11]Free Energy Europe. FEE-14-12C Solar Panel Datasheet. February 2010.  
<http://www.freeenergyeurope.com/pdf/FEE-14-12C-EN.pdf>

[12]Fluke. Pm2811-pm2812-pm2813-pm2831-pm2832 User's Manual, 1997.  
<http://igor.chudov.com/manuals/Fluke-PM2813-User-Manual.pdf>

[13]National Instruments Corporation. Tutorial Getting Started with NI LabVIEW Student Training. June 2010.  
<http://zone.ni.com/devzone/cda/tut/p/id/7466>

[14]Patel, Mukund R. Wind and solar power systems: design, analysis, and operation. Taylor & Francis. 2006. Pages 141-186.

[15]Bishop, Robert H. Learning with LabVIEW 6i. Prentice Hall, 2001.

[16]F.Adamo, F.Attivissimo, M.Spadavecchia. A Tool for Photovoltaic Panels Modeling and Testing. Electrical and Electronic Measurements Laboratory. DEE - Polytechnic of Bari.  
<http://ieeexplore.ieee.org/stamp/stamp.jsp?tp=&arnumber=5488070>

[17]Francisco M.González-Longatt. Model of Photovoltaic Module in Matlab. II CIBELEC 2005)  
[http://personnel.univ-reunion.fr/lanson/typosite/fileadmin/documents/pdf/Heuristiques\\_M2/Projet/lecture\\_ModelPV.pdf](http://personnel.univ-reunion.fr/lanson/typosite/fileadmin/documents/pdf/Heuristiques_M2/Projet/lecture_ModelPV.pdf)

[18]National Instruments Corporation. Tutorial, Photovoltaic Cell I-V Characterization Theory and LabVIEW Analysis Code. December 2009.  
<http://zone.ni.com/devzone/cda/tut/p/id/7230>

[19]Verdiseno, Inc. SolarDesignTool. Compare Solar Panels.  
<http://www.solardesigntool.com/compare-solar-panels-modules.html>

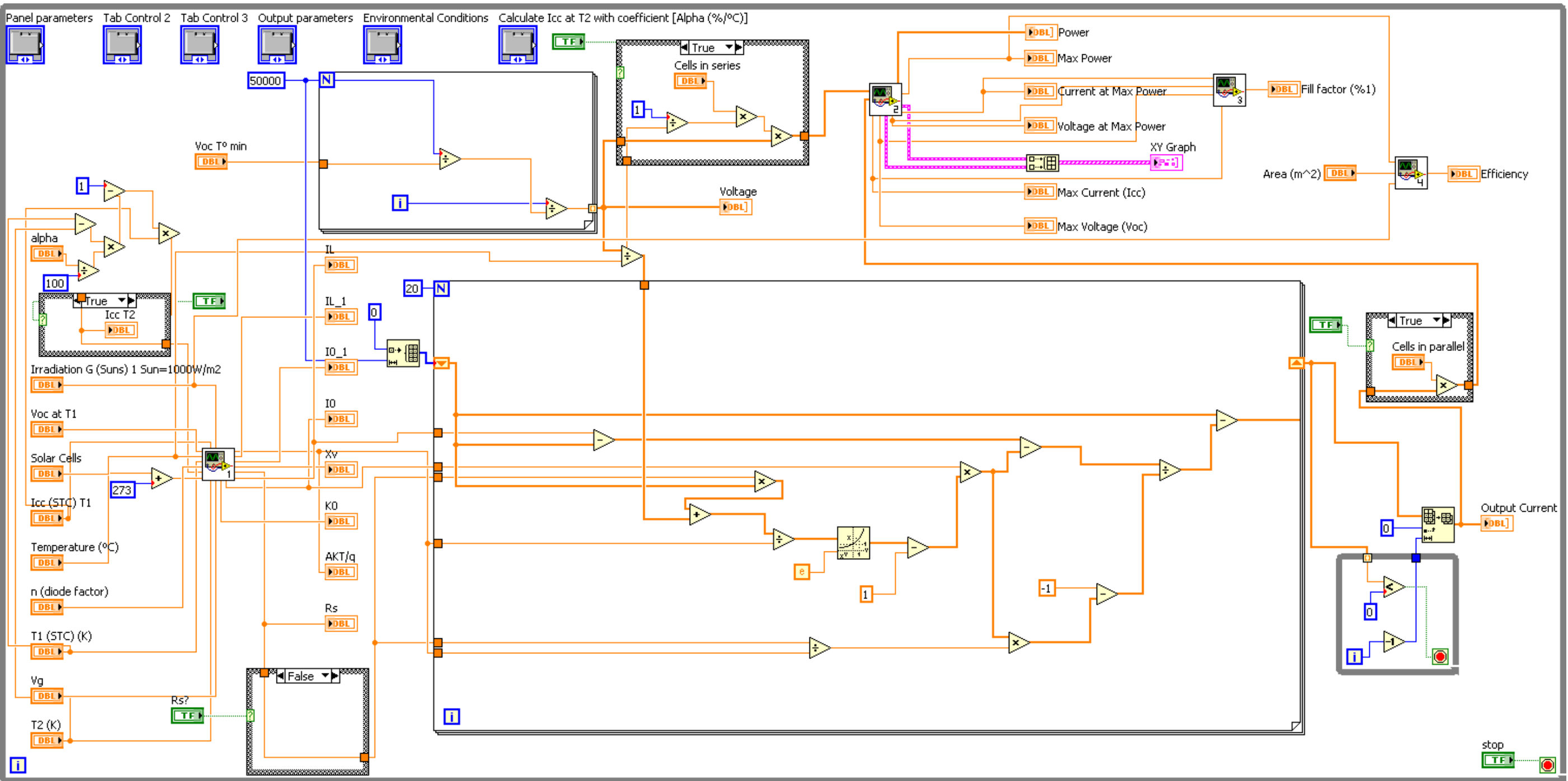
[20]University of Pennsylvania, Department of electrical engineering. Basics of Power Supplies. October 2011.  
<http://www.ese.upenn.edu/detkin/instruments/HPower/PS3631A.html>

[21]National Instruments Corporation. Fluke/Philips flpm28xx Power Supply. LabVIEW Plug and Play Instrument Driver.  
[http://sine.ni.com/apps/utf8/nid\\_web\\_display.download\\_page?p\\_id\\_guid=E3B19B3E920A659CE034080020E74861](http://sine.ni.com/apps/utf8/nid_web_display.download_page?p_id_guid=E3B19B3E920A659CE034080020E74861)

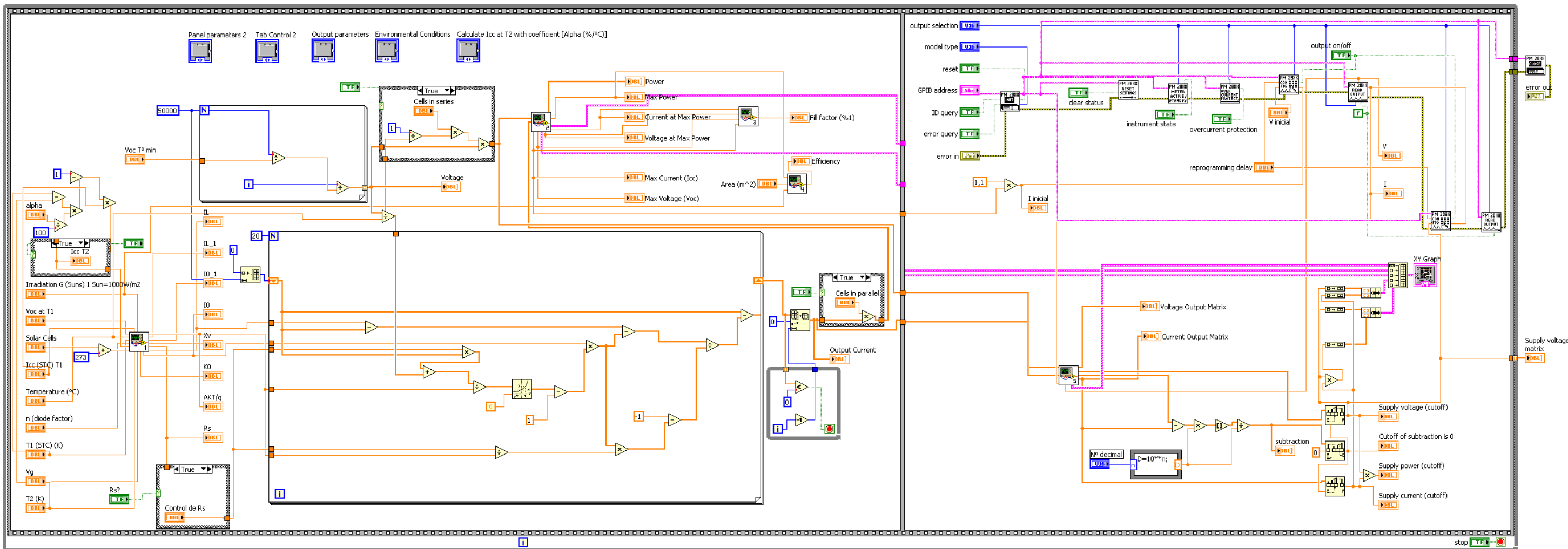
[22]National Instruments Corporation. GPIB-USB-HS Ni-488.2 3.0 driver for windows.  
<http://joule.ni.com/nidu/cds/view/p/id/2706/lang/en>

[23]Isidro Elvis Pereda Soto. Celdas fotovoltaicas en generación distribuida. Pontifical Catholic University of Chile, 2005. Pages 24-43.  
<http://web.ing.puc.cl/~power/paperspdf/pereda.pdf>

## **Annexes**



Annex 1. LabVIEW Block Diagram of “Without Hardware.vi”



## *Annex 2. LabVIEW Block Diagram of “With Hardware.vi”*